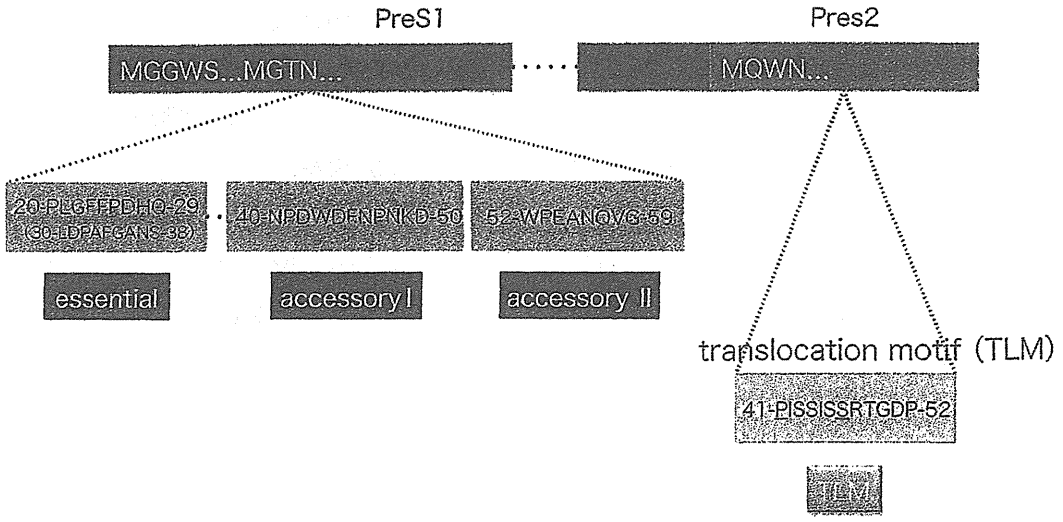

図2　preSの機能配列
preS1内の付着・侵入に必須な機能配列(20～29aa)，付随的機能配列(accessory IおよびII)とpreS2内の侵入過程で重要なTLMを示す．

察されることや，この現象がEGTAで促進される，集団の内部へも感染が確認できるようになる，ことから導き出された．本知見は生体における肝実質細胞の形質は，培養肝癌細胞株に比べ著しい高分化状態にあり，培養肝癌細胞では容易には達成し難い形質を有することを想像させる．この高分化状態がHBV感染レセプターの発現に関わるのか，活性に関わるのか定かではないにせよ，興味深い問題である．

3　付着・融合・侵入に関わるHBV因子

培養肝癌細胞のひとつ，HepG2細胞のHBV感染効率はないに等しいと考える研究者は多いと思われるが，当初はこの細胞を用いたHBV感染粒子の付着機構に関する研究は多々報告された[15,16]．最近ではD型肝炎ウイルス(HDV)なども利用してHepaRG細胞を用いた研究が多い[17]．HBVの感染性粒子の形成には所謂small S（SS若しくは単にHBs)膜蛋白とmiddle S（MS)膜蛋白に加え，large S（LS)膜蛋白が必須の因子となるが，感染性HBV粒子の細胞への付着に関して，特にpreS1領域の機能が重要視されている[18]．preS1領域は部分的にアミノ酸配列の相同性の低いところがあるが，おおむね高い相同性があると考えて良く，付着・膜融合に関わる必須な領域，2つの付随的な領域が存在すると考えられている．preS2領域も相同性は高く，細胞内侵入に関わると思われる領域(translocation motif＝TLM)が想定されている．またSS膜蛋白N末にも膜融合に関わる領域が予測されている．

以上のような情報をもとにして，preS1内の必須領域を介して，肝細胞膜表面因子に結合(付着)し，レセプター分子集合・構造変化，SS膜蛋白N末を加えたHBV粒子膜-細胞膜融合が起こり，TLMを介した細胞内侵入といったHBVの付着・膜融合・侵入機構が想像される．

6　HBV感染レセプターの分離・同定

さて，HBV感染レセプターの分離・同定は倫理的な制約も絡んで，PDH-DHBV系を中心に行われてきた．DHBVにはHBVのMSに相当する膜蛋白はなく，すなわちpreS2に

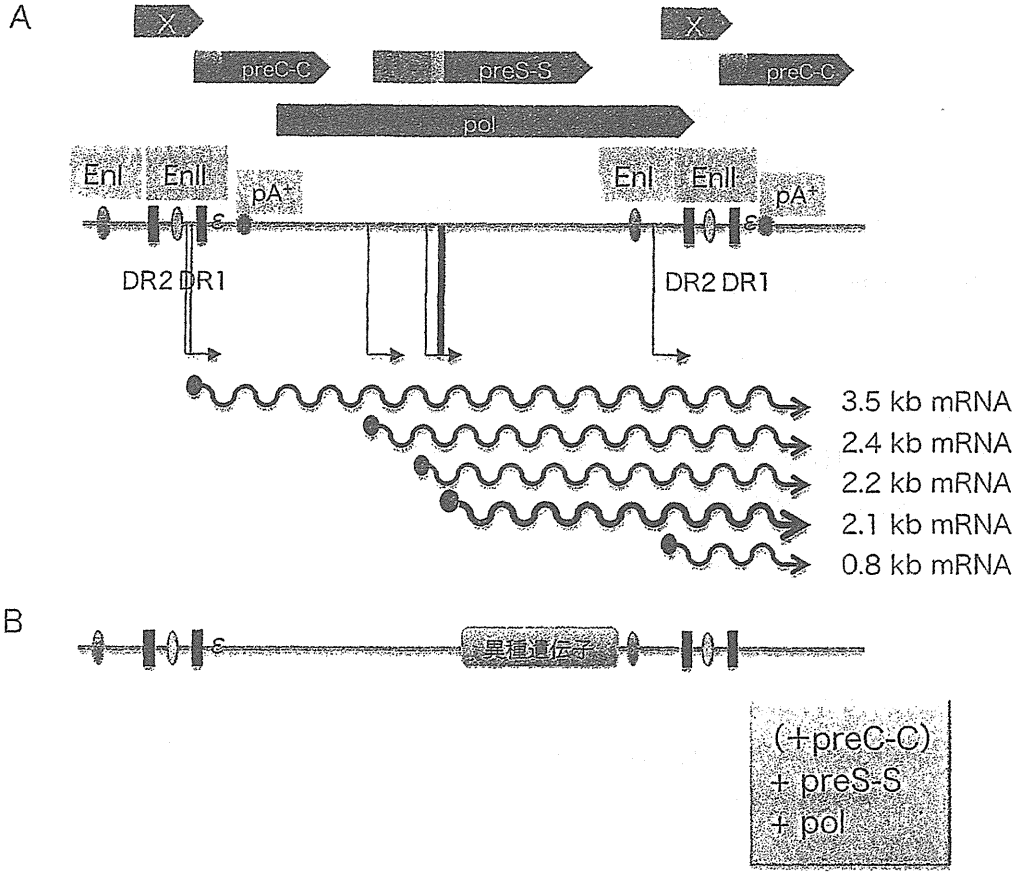

図3　HBVベクター型遺伝子挿入HBVデザイン

A：HBVゲノムを直鎖状に描いている．上段のボックス矢印はORFを示す．pgRNAを発現するための必須基本ユニットを示した．En：エンハンサー．pA：ポリA付加シグナル．鍵矢印は各転写産物の開始部位，波線は転写産物を示す．

B：SSの位置に異種遺伝子を挿入したデザインを示した．この場合，挿入により，preC-C遺伝子，X遺伝子を除くそのほかのHBV関連遺伝子はすべて破壊されるため，トランスに供給する必要がある．挿入部位によってはpreC-Cの供給も必要となる

該当する領域は存在しない．LS内のpreS領域に付着・膜融合に関わる必須な領域，2つのTLMに相当する領域が同定されている．

DHBVで同定された最も有力なDHBV付着因子はgp180（carboxypeptidase D）であった[19]．本因子は膜表面をビオチン化したPDHをDHBVと付着させた後，抗DHBV膜蛋白抗体を用いて免疫沈降することによって分離・同定されたものである．本因子の同定は，HBVの付着・膜融合・侵入に関わるHBV感染レセプターの本質にも迫る因子として期待されたが，LMH細胞(chicken由来の培養肝癌細胞株でDHBV感染を許容しない)をDHBV感染許容細胞へ変化させることはできなかったし，またgp180に対する抗体もアヒル初代培養肝細胞へのDHBV感染を阻止するに至らなかった．

付着因子の存在が報告されているHepG2細胞からもHBV感染が許容される分化誘導したHepaRG細胞からも，依然としてHBV感染レセプターの本体に迫る因子の分離・同定はされていない．現時点における生化学，分子生物学などの技術を駆使しても，確固としたHBV膜蛋白結合因子すらこれらの細胞

から同定されないのはなぜであろうか？ーますますHBV感染レセプターの謎は深まり，逆に興味深くもあるが，HBV感染レセプターの分離・同定には相当の工夫と努力とを余儀なくされると思われる．

7 遺伝子挿入HBVの作製

これまでの経緯から，HBV感染レセプターの分離・同定へ向けた新たな局面を拓くために遺伝子挿入HBV-いわば，組換え型HBV或はpseudotype HBV作製を試みている．この2つの遺伝子挿入HBVは，前者のごとくHBVの複製機構を理解したHBVベクター型か，膜粒子のみをHBV型に変えたpseudotype HBV型に分けられる．本アプローチはこれまでに試みられなかったHBV感染性粒子を基盤にした感染性を指標にするアッセイ系の構築を可能にする．

1. HBVベクター型

本ベクターの構築には，HBVの複製過程を正確に理解する必要がある．HBVは，部分二重鎖DNAという独特のゲノム構造をもつことは勿論，さらに蛋白プライミングによって逆転写複製を行うという極めて特徴的な複製サイクルをもつ[20]．

HBVは感染成立後，部分二重鎖DNAを修復し，いわゆるcccDNAというエピゲノムを形成する．本ゲノムは肝実質細胞核内にあって，転写許容構造体として逆転写の鋳型となる3.5 kbプレゲノムRNAをはじめ，いくつかのHBV関連転写産物産生の鋳型として機能する．3.5 kbプレゲノムRNAはpreC翻訳領域内でDR1（direct repeat 1）を含む形で転写され，3'側にDR2，さらに5'のDR1を含んだやや下流でpolyA付加シグナルが認識されて，すなわち5'と3'が重複される形で集結する．

本稿ではHBV複製サイクルの詳細については省略するが，このベクター構築上最低限必要なエレメントとして，プレゲノムRNA転写開始部位を含めた転写開始装置，5' DR1，ε，DR2，3' DR1配列の基本情報を残しておく必要があり，またどの転写unitを使うか考慮する必要がある（図3A, B）．ウイルス蛋白因子として，実際の逆転写過程から部分二重鎖DNA合成に関わるHBVポリメラーゼ（HBVpol），コア粒子を供給するHBVコア蛋白（HBV-C），膜粒子を構成するpreS-S蛋白（HBV preS-S）を適宜トランスに供給する必要がある（図3B）．またゲノムサイズも厳密に影響すると思われるし，プレゲノムRNAの転写効率を上げるために適宜異種遺伝子エンハンサーを考慮する必要があるかもしれない．

このタイプの遺伝子挿入型HBVはHBVの生活環を踏襲するので，理論上は感染後速やかにcccDNAが形成され遺伝子発現が可能となると予測される．蛍光蛋白遺伝子などで感染をモニターすることにより，HBV感染レセプターの遺伝子の分離・同定に役立てることが可能である．ただし，HBV cccDNAにはγヘルペスウイルスにみられる潜伏感染複製オリジン（ori-P）は存在せず，細胞分裂の際に複製・分配・維持されることなくしだいに希釈されていくと想定される．

私どもは肝実質細胞を標的とした遺伝子治療を達成する目論見で，約20年前に本タイプの遺伝子挿入HBVベクターの開発に挑んだ経緯がある．その後Schallarらを中心として本タイプの遺伝子挿入HBVベクターが作製可能であることが示されている[21]．

2. HBV pseudotype particles（HBVpp）型

このタイプの遺伝子挿入型HBVは，VSV-Gを使ったpantropic retrovirus，あるいはlenti-

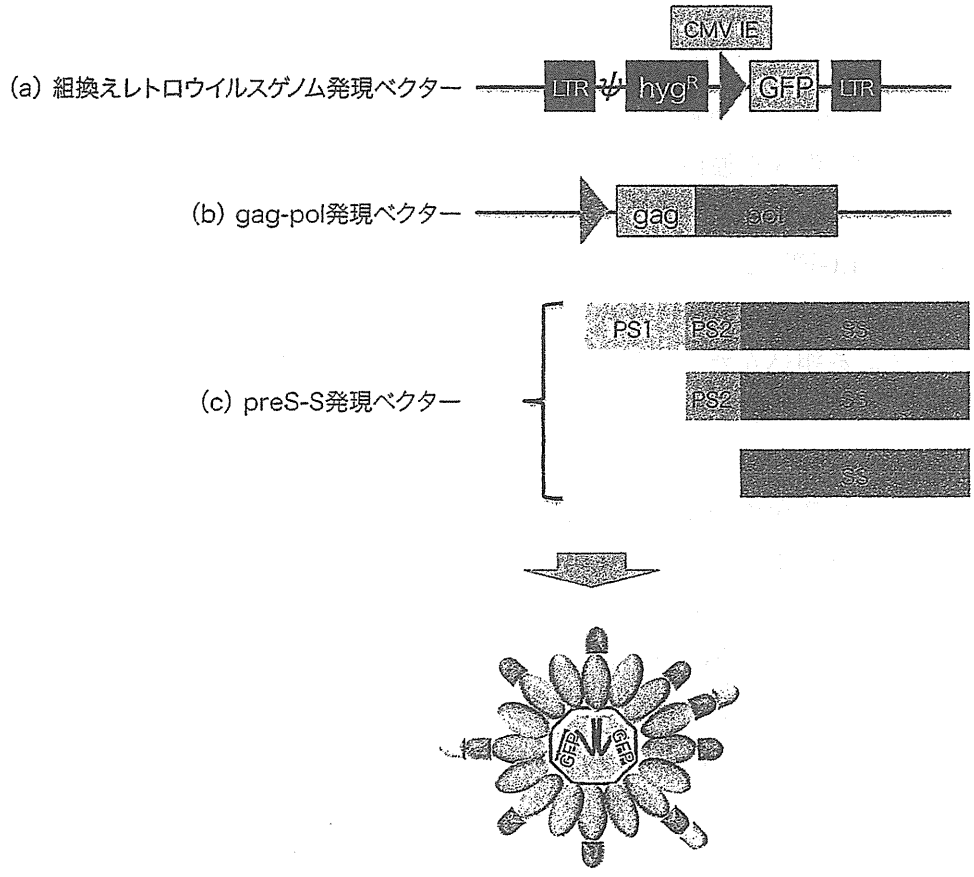

図4　HBVpp型のデザイン

このタイプではレトロウイルスのRNAゲノムを供給する発現ベクター（a），コア粒子と逆転写過程からプロウイルス合成に必要なpolを供給するgag-pol発現ベクター，HBV膜粒子を供給するHBVの3つの膜蛋白を供給する発現ベクターが必要となる．(b)にHIV型を用い，(a)にHIV（レンチウイルス）型のゲノムを供するrev responsive element（RRE）などの必要なエレメントを携えておけば，レンチウイルス型のレトロウイルスベクターとなる．(a)あるいは(b)をあらかじめ安定型培養細胞株として樹立してパッケージング細胞として使用することも可能である．LTR: long terminal repeat. hyg^R: hygromycine resistance gene. CMV IE: cytomegalovirus immediate early enhancer-promoter. GFP: green fluorescent protein. ψ：レトロウイルスパッケージングシグナル．▷：エンハンサー-プロモーター．

virusにおいてVSV-GをHBV膜蛋白に変えたpseudo-HBVである．HCVでもpseudotype particles（HCVpp）として試みられている[22]．HBVppは付着・侵入はHBVの過程を辿り，それ以降の過程はレトロウイルスの生活環に従う．最終的には逆転写過程を経て，プロウイルスとして安定的に感染宿主細胞ゲノムに組み込まれるので，培養細胞など，継代が基本的に可能な細胞を用いた場合，ウイルス遺伝子として蛍光蛋白遺伝子や薬剤耐性遺伝子を挿入しておけば，感染細胞はクローン化できることになる．

問題となるのは，通常のレトロウイルスベクターを用いた場合，感染後，プロウイルスを形成し，安定的な挿入遺伝子の発現まで数日から1週間程度の時間を要する点である．この意味でlentivirus型のレトロウイルスをベースにしたHBVppが望ましいかもしれない．

私どもの研究室では，肝実質細胞のcDNA

ライブラリーを培養肝癌細胞へ導入後，HBVppの感染性を指標にしたHBV感染レセプターの分離・同定を試みる戦略で通レトロウイルス型HBVppの構築を独自に試みた．まずレトロウイルスのgag-pol遺伝子を発現する細胞にEGFP（EGFP）とハイグロマイシン耐性遺伝子(HygR)を挿入したレトロウイルスベクターゲノムを組込んだパッケージング細胞を作製し，この細胞に3つのHBV膜蛋白を発現させることで培養上清中にHBV膜蛋白を被ったウイルス粒子が産生されるかどうかを検討した．抗HBs抗体による免疫沈降，ウイルスゲノム抽出，RT-PCRで免疫沈降したサンプルに挿入したEGFP遺伝子が確認された．セシウム密度勾配超遠心法でもHBV粒子密度に近い1.22 g/m*l*近傍に粒子が集積することや，電顕によっても粒子形成されていることが確認された[23]．なお，本HBVppの感染能についていくつかの知見を得ているが本稿では差し控えたい．

8 おわりに

以上，遺伝子挿入HBVベクターについて概説した．HBVベクタータイプもHBVppタイプも作製可能であり，それぞれの利点を活かしたHBV感染レセプターの分離・同定における利用価値は高いと思われる．またこれら2つの遺伝子挿入HBVベクターは感染性を指標にしたアッセイ系を組み立てることにより，HBV感染レセプター分離・同定後の*in vitro*，および*in vivo*におけるHBV生活環や病態解析解明，治療法の開発とその評価系の構築に有用性は極めて高いものと思われる．

文　献

1) Blumberg BS, Alter HJ, Visnich S : A "New" Antigen in Leukemia Sera. JAMA 191 : 541–546, 1965
2) Seeger C, Zoulim F, MASON WS : Hepadnaviruses. In "Fields Viriology". 5th ed , 2007, pp2977–3029
3) Funk A, Mhamdi M, Will H et al : Avian hepatitis B viruses: molecular and cellular biology, phylogenesis, and host tropism. World J Gastroenterol 13 : 91–103, 2007
4) Menne S, Cote PJ : The woodchuck as an animal model for pathogenesis and therapy of chronic hepatitis B virus infection. World J Gastroenterol 13 : 104–124, 2007
5) Hellström U, Sylvan S : Human serum albumin and the enigma of chronic hepatitis type B. Scand J Immunol 23 : 523–527, 1986
6) Li JS, Tong SP, Wands JR : Characterization of a 120-Kilodalton pre-S-binding protein as a candidate duck hepatitis B virus receptor. J Virol 70 : 6029–6035, 1996
7) Kuroki K, Cheung R, Marion PL et al : A cell surface protein that binds avian hepatitis B virus particles. J Virol 68 : 2091–2096, 1994
8) Tsurimoto T, Fujiyama A, Matsubara K : Stable expression and replication of hepatitis B virus genome in an integrated state in a human hepatoma cell line transfected with the cloned viral DNA. Proc Natl Acad Sci USA 84 : 444–448, 1987
9) Sells MA, Chen ML, Acs G : Production of hepatitis B virus particles in Hep G2 cells transfected with cloned hepatitis B virus DNA. Proc Natl Acad Sci USA 84 : 1005–1009, 1987
10) Bchini R, Capel F, Dauguet C et al : In vitro infection of human hepatoma (HepG2) cells with hepatitis B virus. J Virol 64 : 3025–3032, 1990
11) Gripon P, Rumin S, Urban S et al : Infection of a human hepatoma cell line by hepatitis B virus. Proc Natl Acad Sci USA 99 : 15655–15660, 2002
12) Hantz O, Parent R, Durantel D et al : Persistence of the hepatitis B virus covalently closed circular DNA in HepaRG human hepatocyte-like cells. J Gen Virol 90 : 127–135, 2009
13) Marion MJ, Hantz O, Durantel D : The HepaRG cell line: biological properties and relevance as a tool for cell biology, drug metabolism, and virology studies. Methods Mol Biol 640 : 261–272, 2010
14) Schulze A, Mills K, Weiss TS et al : Hepatocyte

polarization is essential for the productive entry of the hepatitis B virus. Hepatology 55 : 373–383, 2012
15) Neurath AR, Kent SB, Strick N et al : Identification and chemical synthesis of a host cell receptor binding site on hepatitis B virus. Cell 46 : 429–436, 1986
16) Petit MA, Dubanchet S, Capel F et al : HepG2 cell binding activities of different hepatitis B virus isolates: inhibitory effect of anti-HBs and anti-preS1 (21-47). Virology 180 : 483–491, 1991
17) Blanchet M, Sureau C : Analysis of the cytosolic domains of the hepatitis B virus envelope proteins for their function in viral particle assembly and infectivity. J Virol 80 : 11935–11945, 2006
18) Glebe D, Urban S : Viral and cellular determinants involved in hepadnaviral entry. World J Gastroenterol 13 : 22–38, 2007
19) Kuroki K, Eng F, Ishikawa T et al : gp180, a host cell glycoprotein that binds duck hepatitis B virus particles, is encoded by a member of the carboxypeptidase gene family. J Biol Chem 270 : 15022–15028, 1995
20) Beck J, Nassal M : Hepatitis B virus replication. World J Gastroenterol 13 : 48–64, 2007
21) Protzer U, Nassal M, Chiang PW et al : Interferon gene transfer by a hepatitis B virus vector efficiently suppresses wild-type virus infection. Proc Natl Acad Sci USA 96 : 10818–10823, 1999
22) Evans MJ, von Hahn T, Tscherne DM et al : Claudin-1 is a hepatitis C virus co-receptor required for a late step in entry. Nature 446 : 801–805, 2007
23) Ueda K, Ohsaki E, Omori H : submitted.

*　　*　　*

PLOS ONE

Inhibition of Both Protease and Helicase Activities of Hepatitis C Virus NS3 by an Ethyl Acetate Extract of Marine Sponge *Amphimedon* sp.

Yuusuke Fujimoto[1], Kazi Abdus Salam[2☯], Atsushi Furuta[3,4☯], Yasuyoshi Matsuda[3,4], Osamu Fujita[3,4], Hidenori Tani[5], Masanori Ikeda[6], Nobuyuki Kato[6], Naoya Sakamoto[7], Shinya Maekawa[8], Nobuyuki Enomoto[8], Nicole J. de Voogd[9], Masamichi Nakakoshi[10], Masayoshi Tsubuki[10], Yuji Sekiguchi[3], Satoshi Tsuneda[4], Nobuyoshi Akimitsu[2], Naohiro Noda[3,4], Atsuya Yamashita[1]*, Junichi Tanaka[11]*, Kohji Moriishi[1]*

1 Department of Microbiology, Division of Medicine, Graduate School of Medicine and Engineering, University of Yamanashi, Yamanashi, Japan, **2** Radioisotope Center, The University of Tokyo, Tokyo, Japan, **3** Biomedical Research Institute, National Institute of Advanced Industrial Science and Technology, Ibaraki, Japan, **4** Department of Life Science and Medical Bioscience, Waseda University, Tokyo, Japan, **5** Research Institute for Environmental Management Technology, National Institute of Advanced Industrial Science and Technology, Ibaraki, Japan, **6** Department of Tumor Virology, Okayama University Graduate School of Medicine, Dentistry, and Pharmaceutical Sciences, Okayama, Japan, **7** Department of Gastroenterology and Hepatology, Hokkaido University Graduate School of Medicine, Sapporo, Japan, **8** First Department of Internal Medicine, Faculty of Medicine, University of Yamanashi, Yamanashi, Japan, **9** Netherlands Centre for Biodiversity Naturalis, Leiden, The Netherlands, **10** Institute of Medical Chemistry, Hoshi University, Tokyo, Japan, **11** Department of Chemistry, Biology and Marine Science, University of the Ryukyus, Okinawa, Japan

Abstract

Combination therapy with ribavirin, interferon, and viral protease inhibitors could be expected to elicit a high level of sustained virologic response in patients infected with hepatitis C virus (HCV). However, several severe side effects of this combination therapy have been encountered in clinical trials. In order to develop more effective and safer anti-HCV compounds, we employed the replicon systems derived from several strains of HCV to screen 84 extracts from 54 organisms that were gathered from the sea surrounding Okinawa Prefecture, Japan. The ethyl acetate-soluble extract that was prepared from marine sponge *Amphimedon* sp. showed the highest inhibitory effect on viral replication, with EC_{50} values of 1.5 and 24.9 μg/ml in sub-genomic replicon cell lines derived from genotypes 1b and 2a, respectively. But the extract had no effect on interferon-inducing signaling or cytotoxicity. Treatment with the extract inhibited virus production by 30% relative to the control in the JFH1-Huh7 cell culture system. The *in vitro* enzymological assays revealed that treatment with the extract suppressed both helicase and protease activities of NS3 with IC_{50} values of 18.9 and 10.9 μg/ml, respectively. Treatment with the extract of *Amphimedon* sp. inhibited RNA-binding ability but not ATPase activity. These results suggest that the novel compound(s) included in *Amphimedon* sp. can target the protease and helicase activities of HCV NS3.

Citation: Fujimoto Y, Salam KA, Furuta A, Matsuda Y, Fujita O, et al. (2012) Inhibition of Both Protease and Helicase Activities of Hepatitis C Virus NS3 by an Ethyl Acetate Extract of Marine Sponge *Amphimedon* sp.. PLoS ONE 7(11): e48685. doi:10.1371/journal.pone.0048685

Editor: Tetsuo Takehara, Osaka University Graduate School of Medicine, Japan

Received June 16, 2012; **Accepted** October 1, 2012; **Published** November 7, 2012

Funding: This work was supported in part by grants-in-aid from the Ministry of Health, Labor, and Welfare (http://www.mhlw.go.jp/) and from the Ministry of Education, Culture, Sports, Science, and Technology of Japan (http://www.mext.go.jp/). The funders had no role in study design, data collection and analysis, decision to publish, or preparation of the manuscript.

Competing Interests: The authors have declared that no competing interests exist.

* E-mail: atsuyay@yamanashi.ac.jp (AY); jtanaka@sci.u-ryukyu.ac.jp (JT); kmoriishi@yamanashi.ac.jp (KM)

☯ These authors contributed equally to this work.

Introduction

Hepatitis C virus (HCV) is an enveloped RNA virus of the genus *Hepacivirus* of the *Flaviviridae* family. More than 170 million patients persistently infected with HCV have been reported worldwide, leading to liver diseases including steatosis, cirrhosis, and hepatocellular carcinoma [1,2]. The genome of HCV is characterized as a single positive-strand RNA with a nucleotide length of 9.6 kb, flanked by 5′ and 3′-untranslated regions (UTRs). The genomic RNA encodes a large polyprotein consisting of approximately 3,000 amino acids [3], which is translated under the control of an internal ribosome entry site (IRES) located within the 5′-UTR of the genomic RNA [4]. The translated polyprotein is cleaved by host and viral proteases, resulting in 10 mature viral proteins [3]. The structural proteins, consisting of core, E1, and E2, are located in the N-terminal quarter of the polyprotein, followed by viroporin p7, which has not yet been classified into a structural or nonstructural protein. Further cleavage of the remaining portion by viral proteases produces six nonstructural proteins–NS2, NS3, NS4A, NS4B, NS5A, and NS5B–which form a viral replication complex with various host factors. The viral protease NS2 cleaves its own C-terminal between NS2 and NS3. After that, NS3 cleaves the C-terminal ends of NS3 and NS4A and then forms a complex with NS4A. The NS3/4A complex becomes a fully active form to cleave the C-terminal parts of the polyprotein, including nonstructural proteins. NS3 also possesses

RNA helicase activity to unwind the double-stranded RNA during the synthesis of genomic RNA [5,6].

Although the previous standard therapy, combining pegylated interferon with ribavirin, was effective in only about half of patients infected with genotype 1, the most common genotype worldwide [7–9], recent biotechnological advances have led to the development of a novel therapy using anti-HCV agents that directly target HCV proteins or host factors required for HCV replication and have improved the sustained virologic response (SVR) [10–12]. Telaprevir and boceprevir, which are categorized as advanced NS3/4A protease inhibitors, were recently approved for the treatment of chronic hepatitis C patients infected with genotype 1 [13,14]. The triple combination therapy with pegylated interferon, ribavirin, and telaprevir improved SVR by 77% in patients infected with genotype 1 [15]. However, this therapy exhibits side effects including rash, severe cutaneous eruption, influenza-like symptoms, cytopenias, depression, and anemia [7,16,17]. Furthermore, the possibility of the emergence of drug-resistant viruses is a serious problem with therapies that use antiviral compounds [18,19].

Recent technical advances in the determination of molecular structures and the synthesis of chemical compounds have led to the development of various drugs based on natural products, especially drugs identified from terrestrial plants and microbes [20–22]. Marine organisms, including plants and animals, were recently established as representative of a natural resource library for drug development. Potent biological activity is often found in products isolated from marine organisms because of their novel molecular structures [23,24]. Trabectedin (Yondelis), cytarabine (Ara-C), and eribulin (Halaven), which are known as antitumor drugs, were developed from compounds found in marine organisms [25].

In this study, we screened 84 extracts prepared from 54 marine organisms by using replicon cell lines derived from HCV genotype 1b and attempted to identify the extract that inhibits HCV RNA replication. A marine organism may produce anti-HCV agent(s) that could inhibit the protease and helicase activities of NS3.

Results

Effect of the Extract from Marine Sponge and Tunicate on HCV Replication

We prepared methanol (MeOH)- and ethyl acetate (EtOAc)-soluble extracts from 54 marine organisms in order to test which of these extracts could best suppress HCV replication. Each extract was added at 25 μg/ml to the culture supernatant of HCV replicon cell lines derived from O and Con1 strains of genotype 1b, which produce the luciferase/neomycin hybrid protein depending on RNA replication. Luciferase activity and cell viability were measured 72 h after treatment with the extracts (Table 1). The extracts exhibiting more than 85% cell viability and lower than 15% luciferase activity were selected as arbitrary candidates for the extract including anti-HCV compounds. The EtOAc-extract prepared from sample C-29 (C-29EA) was selected as a candidate in both cell lines. Thus, the anti-HCV activity of extract C-29EA was tested.

The EtOAc-soluble extract C-29EA was prepared from the marine sponge *Amphimedon* sp. (Fig. 1A), which inhabits the sea surrounding Okinawa Prefecture, Japan. HCV replication was inhibited in a dose-dependent manner but did not exhibit cytotoxicity when replicon cells were treated with C-29EA (Fig. 1 B). The extract C-29EA exhibited EC_{50} values of 1.5 μg/ml (Table 2). Furthermore, treatment with C-29EA suppressed the HCV replication derived from the genotype 2a strain JFH1 with an EC_{50} of 24.9 μg/ml, irrespective of cell viability (Fig. 2A and Table 2). Extract C-29EA also inhibited the production of infectious viral particles, viral RNA, and core protein from JFH1-infected cells in the supernatant (Fig. 2B and C). These results suggest that the marine sponge *Amphimedon* sp. possesses anti-HCV agents.

Effect of Extract C-29EA on IRES-dependent Translation

Extract C-29EA had the most potent inhibitory activity against HCV replication. The viral replication (Fig. 1 B and 2 A) and viral proteins (Fig. 3 A and B) in replicon cell lines derived from genotype 1b strain Con1 and 2a strain JFH1 were decreased 72 h after treatment in a dose-dependent manner. HCV protein has been translated based on the positive-sense viral RNA in an IRES-dependent manner. The replicon RNA of HCV is composed of the 5′-UTR of HCV, indicator genes (a luciferase-fused drug-resistant gene), encephalomyocarditis virus (EMCV) IRES, the viral genes encoding complete or nonstructural proteins, and the 3′-UTR of HCV, in that order [26]. The replicon RNA replicated autonomously in several HCV replication-permissive cell lines derived from several hepatoma cell lines. Nonstructural proteins in replicon cells were polycistronically translated through EMCV IRES. The cap-dependent translated mRNA, including *Renilla* luciferase, EMCV IRES, and the firefly luciferase/neomycin-resistant gene, in that order, was constructed to examine the effect of the extract on EMCV-IRES-dependent translation (Fig. 3C). When the mRNA expression was transcribed by an EF promoter of the transfected plasmid in the presence of C-29EA, the ratio of firefly luciferase activity to *Renilla* luciferase activity was not changed (Fig. 3C). This suggested that treatment with C-29EA exhibited no effect on EMCV-IRES-dependent translation. Furthermore, treatment with C-29EA did not significantly affect the activity of HCV IRES that was used instead of EMCV IRES in the system described above (Fig. 3D). Thus, these results suggest that treatment with C-29EA exhibits no effect on EMCV- or HCV-IRES-dependent translation.

Effect of C-29EA on the Interferon Signaling Pathway

It has been well known that HCV replication in cultured cells is potently inhibited by interferon [27,28]. We examined whether or not treatment with C-29EA elicits an interferon-inducible gene from replicon cells. The replicon cells were treated with various concentrations of interferon-alpha 2b or 15 μg of C-29EA per milliliter. The treated cells were harvested at 72 h post-treatment. The interferon-inducible gene 2′, 5′-OAS, was induced with IFN-alpha 2b but not with a 10-times EC_{50} concentration of C-29EA (Fig. 4). These results suggest that the inhibitory effect of C-29EA on the replication of the HCV replicon is independent of the IFN signaling pathway.

Effect of C-29EA on the NS3 Helicase Activity

We previously established an assay system for unwinding HCV activity based on photoinduced electron transfer (PET) [29,30]. The fluorescent dye (BODIPY FL) is attached to the cytosine at the 5′-end of the fluorescent strand and quenched by the guanine base at the 3′-end of the complementary strand via PET. When helicase unwinds the double-strand RNA substrate, the fluorescence of the dye emits a bright light upon the release of the dye from the guanine base. The capture strand, which is complementary to the complementary strand, prevents the reannealing of the unwound duplex. Treatment with C-29EA inhibited the helicase activity in a dose-dependent manner, with an IC_{50} value of 18.9 μg/ml (Fig. 5A). We confirmed the effect of C-29EA on NS3 helicase unwinding activity by the RNA helicase assay using ^{32}P-labeled double-stranded RNA (dsRNA) as a substrate. Treatment

Table 1. Effect of marine organism extracts on HCV replication and cell viability.

No.	Sample	Luciferase activity (% of control)		Cell viability (% of control)		Phylum	Specimen	Extract	Site
		O	Con1	O	Con1				
1	A-1	10	111	105	104	Sponge	*Unidentified*	MeOH	A
2	A-2	82	209	91	132	Soft coral	*Briareum*	MeOH	A
3	A-3	87	177	54	110	Tunicate	*unidentified*	MeOH	A
4	A-4	82	186	84	100	Sponge	*Liosina*	MeOH	A
5	B-5	110	165	86	110	Sponge	*unidentified*	MeOH	B
6	B-6	70	149	103	119	Sponge	*Xestospongia*	MeOH	B
7	B-7	89	191	111	144	Sponge	*Epipolasis*	MeOH	B
8	B-8	89	182	115	132	Sponge	*unidentified*	MeOH	B
9	B-9	57	72	92	124	Sponge	*Strongylophora*	MeOH	B
10	B-10	106	182	73	96	Sponge	*Stylotella aurantium*	MeOH	B
11	C-12	96	162	114	98	Sponge	*Epipolasis*	MeOH	B
12	C-13	123	141	91	103	Sponge	*unidentified*	MeOH	B
13	C-14	89	175	77	100	Sponge	*Hippospongia*	MeOH	B
14	C-16	80	177	108	88	Sponge	*unidentified*	MeOH	B
15	C-18	119	170	93	94	Sponge	*unidentified*	MeOH	B
16	C-19	0	0	0	4	Sponge	*unidentified*	MeOH	B
17	C-20	101	158	61	106	Sponge	*Xestospongia testudinaria*	MeOH	B
18	C-21	85	161	83	102	Sponge	*unidentified*	MeOH	B
19	C-22	109	88	38	89	Sponge	*unidentified*	MeOH	B
20	C-23	94	156	32	90	Sponge	*unidentified*	MeOH	B
21	C-24	118	86	42	94	Sponge	*Theonella*	MeOH	B
22	C-25	82	111	91	106	Sponge	*unidentified*	MeOH	B
23	C-27	0	0	15	2	Sponge	*unidentified*	MeOH	B
24	C-28	90	166	30	90	Sponge	*Petrosia*	MeOH	B
25	C-29	65	151	29	101	Sponge	*Amphimedon*	MeOH	B
26	D-31	81	127	55	91	Tunicate	*unidentified*	MeOH	C
27	D-32	80	141	47	93	Sponge	*unidentified*	MeOH	C
28	D-33	88	153	72	90	Gorgonian	*Junceella fragilis*	MeOH	C
29	E-35	114	156	40	118	Sponge	*Phyllospongia sp.*	MeOH	C
30	E-36	80	125	69	116	Tunicate	*Didemnum molle*	MeOH	C
31	E-37	88	129	54	108	Sponge	*Xestospongia sp.*	MeOH	C
32	E-38	70	153	35	112	Sponge	*unidentified*	MeOH	C
33	F-40	119	170	38	104	Sponge	*unidentified*	MeOH	C
34	F-41	88	166	48	101	Soft coral	*unidentified*	MeOH	C
35	G-42	113	157	31	126	Sponge	*unidentified*	MeOH	D
36	H-43	83	0	39	5	Sponge	*unidentified*	MeOH	D
37	J-44	62	183	27	105	Sponge	*Cinachyra*	MeOH	D
38	J-45	96	140	47	103	Sponge	*Liosina*	MeOH	D
39	J-46	83	149	77	102	Sponge	*unidentified*	MeOH	D
40	J-47	94	37	40	111	Sponge	*unidentified*	MeOH	D
41	J-48	24	16	53	70	Sponge	*Stylotella*	MeOH	D
42	J-49	78	123	55	105	Sponge	*unidentified*	MeOH	D
43	J-50	93	138	51	108	Sponge	*unidentified*	MeOH	D
44	J-51	103	73	41	115	Sponge	*unidentified*	MeOH	D
45	J-52	162	237	113	131	Sponge	*unidentified*	MeOH	D
46	J-53	51	90	93	122	Tunicate	*Didemnum*	MeOH	D
47	J-54	42	90	113	124	Sponge	*unidentified*	MeOH	D

Table 1. Cont.

No.	Sample	Luciferase activity (% of control)		Cell viability (% of control)		Phylum	Specimen	Extract	Site
		O	Con1	O	Con1				
48	J-55	88	133	131	110	Jellyfish	*unidentified*	MeOH	D
49	J-56	28	51	113	103	Sponge	*unidentified*	MeOH	D
50	J-57	8	63	94	85	Tunicate	*Pseudodistoma kanoko*	MeOH	D
51	J-58	0	2	48	65	Sponge	*unidentified*	MeOH	D
52	J-59	0	2	45	71	Sponge	*unidentified*	MeOH	D
53	J-60	98	134	122	95	Annelid	*unidentified*	MeOH	D
54	A-2	0	1	6	15	Soft coral	*Briareum*	EtOAc	A
55	A-3	0	0	6	9	Tunicate	*unidentified*	EtOAc	A
56	A-4	22	36	74	76	Sponge	*Liosina*	EtOAc	A
57	B-5	33	107	69	93	Sponge	*unidentified*	EtOAc	B
58	B-6	0	0	5	8	Sponge	*Xestospongia*	EtOAc	B
59	B-7	0	0	5	9	Sponge	*Epipolasis*	EtOAc	B
60	B-8	0	0	2	46	Sponge	*unidentified*	EtOAc	B
61	B-9	0	0	8	14	Sponge	*Strongylophora*	EtOAc	B
62	B-10	0	0	3	8	Sponge	*Stylotella aurantium*	EtOAc	B
63	C-12	0	0	4	14	Sponge	*Epipolasis*	EtOAc	B
64	C-13	0	0	4	5	Sponge	*unidentified*	EtOAc	B
65	C-14	48	119	82	102	Sponge	*Hippospongia*	EtOAc	B
66	C-15	0	0	8	11	Sponge	*unidentified*	EtOAc	B
67	C-18	0	0	4	3	Sponge	*unidentified*	EtOAc	B
68	C-19	23	76	63	109	Sponge	*unidentified*	EtOAc	B
69	C-20	34	32	63	112	Sponge	*Xestospongia testudinaria*	EtOAc	B
70	C-21	1	0	52	12	Sponge	*unidentified*	EtOAc	B
71	C-22	76	34	74	110	Sponge	*unidentified*	EtOAc	B
72	C-24	0	0	20	7	Sponge	*Theonella*	EtOAc	B
73	C-26	41	43	80	110	Sponge	*unidentified*	EtOAc	B
74	C-27	1	0	35	40	Sponge	*unidentified*	EtOAc	B
75	C-28	68	62	82	115	Sponge	*Petrosia*	EtOAc	B
76	C-29	10	11	93	88	Sponge	*Amphimedon*	EtOAc	B
77	D-31	20	71	85	120	Tunicate	*Eudistoma*	EtOAc	C
78	D-33	0	0	5	7	Gorgonian	*Junceella fragilis*	EtOAc	C
79	E-35	0	0	4	5	Sponge	*Phyllospongia sp.*	EtOAc	C
80	E-36	71	83	75	100	Tunicate	*Didemnum molle*	EtOAc	C
81	F-40	72	110	87	130	Sponge	*unidentified*	EtOAc	C
82	F-41	8	33	73	104	Soft coral	*unidentified*	EtOAc	C
83	H-43	0	197	4	119	Sponge	*unidentified*	EtOAc	D
84	J-46	113	58	103	126	Sponge	*unidentified*	EtOAc	D

There are a total of 54 marine organisms, while 84 extracts were prepared from them with ethyl acetate and/or methanol. Aragusuku, Iriomote, Kohama, and Ishigaki islands are indicated by A, B, C, and D, respectively, in the collection-site column?(right end). EtOAc: Ethyl acetate; MeOH: Methanol.

doi:10.1371/journal.pone.0048685.t001

with C-29EA inhibited dsRNA dissociation at a concentration of 16 μg/ml and above (Fig. 5B).

The unwinding ability of HCV helicase depends on ATP binding, ATP hydrolysis, and RNA binding [30,31]. We examined the effect of C-29EA on the ATPase activity of NS3. The ratio of free phosphate (^{32}P-Pi) to ATP (^{32}P-ATP) was determined in the presence of C-29EA. The reaction was carried out between 16 and 250 μg of C-29EA per milliliter. The ATPase activity of NS3 helicase was not inhibited (Fig. 6A), although the helicase activity was decreased to less than 20% in the presence of 50 μg of C-29EA per milliliter (Fig. 5A). Next, we examined the effect of C-29EA on the binding of NS3 helicase to single-strand RNA (ssRNA). A gel-mobility shift assay was employed to estimate the binding activity of NS3 to the 21-mer of ssRNA. The binding of NS3 to ssRNA was inhibited by C-29EA in a dose-dependent manner (Fig. 6 B and C). These results suggest that treatment with C-29EA inhibits the helicase activity of NS3 by suppressing RNA binding.

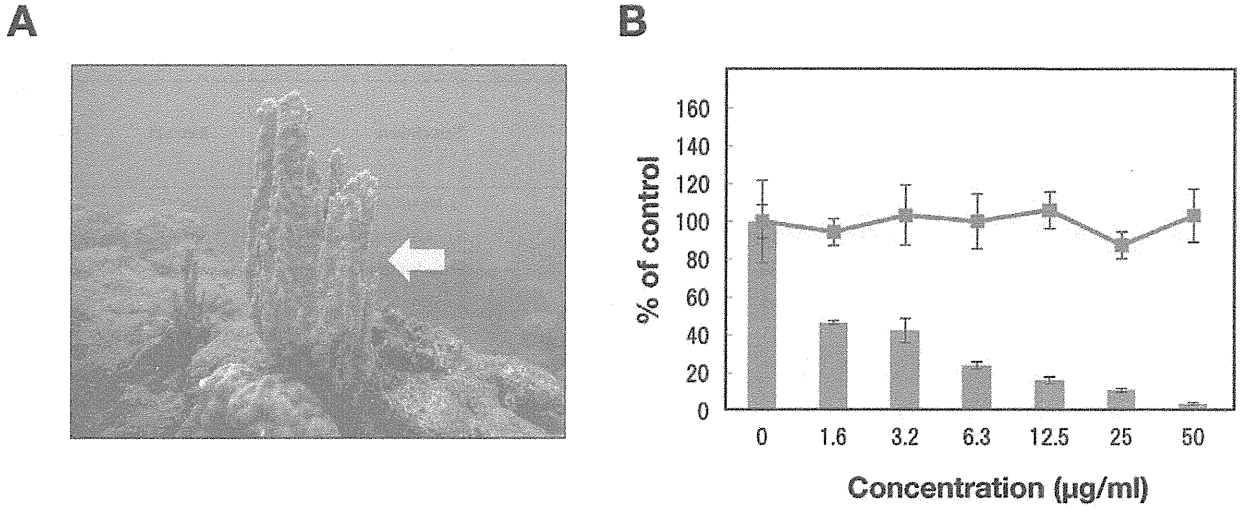

Figure 1. Effect of the extract prepared from a marine sponge on viral replication in the replicon cell line derived from viral genotype 1b. (A) *Amphimedon* sp. belongs to a marine sponge. The ethyl acetate fraction prepared from the marine organism was designated C-29EA in this study. (B) The Huh7 cell line, including the subgenomic replicon RNA of genotype 1b strain Con1, was incubated in medium containing various concentrations of C-29EA or DMSO (0). Luciferase and cytotoxicity assays were carried out as described in Materials and Methods. Error bars indicate standard deviation. The data represent three independent experiments.
doi:10.1371/journal.pone.0048685.g001

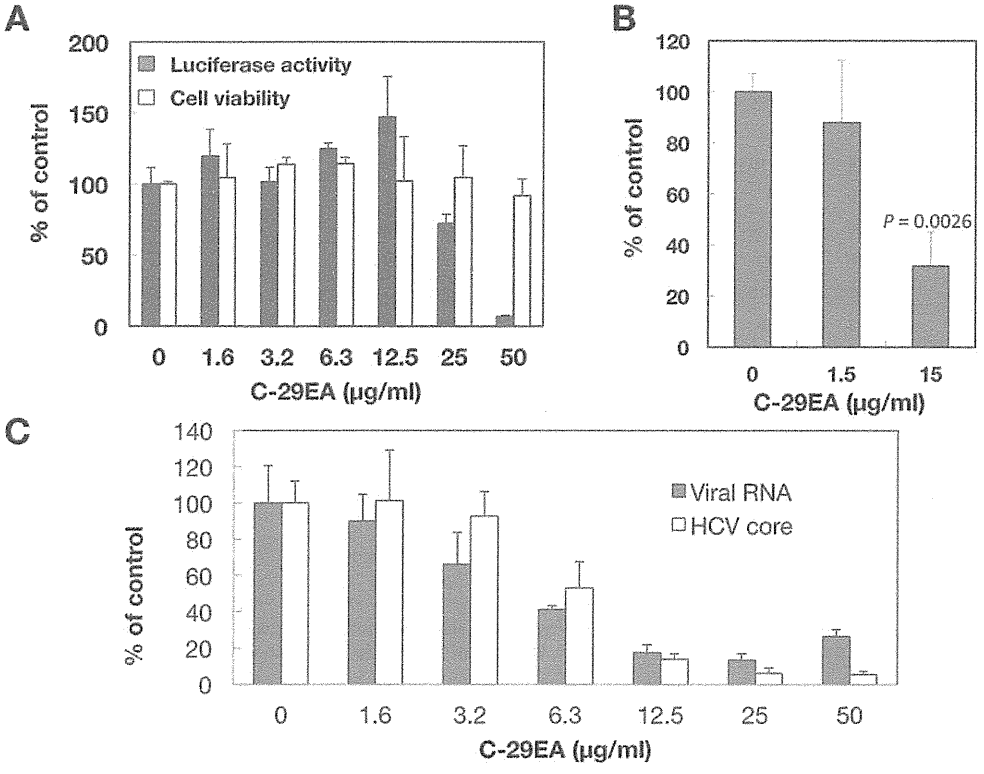

Figure 2. Effect of C-29EA extract on viral replication in the replicon cell line derived from viral genotype 2a. (A) The Huh7 cell line, including the subgenomic replicon RNA of genotype 2a strain JFH1, was incubated in medium containing various concentrations of C-29EA or DMSO (0). Luciferase and cytotoxicity assays were carried out as described in Materials and Methods. (B) The Huh7 OK1 cell line infected with HCVcc JFH1 was incubated with various concentrations of C-29EA or DMSO (0). The virus titers were determined by a focus-forming assay. The significance of differences in the means was determined by Student's *t*-test. (C) Amounts of viral RNA and core protein were estimated by qRT-PCR and ELISA, respectively. Error bars indicate standard deviation. The data represent three independent experiments. Treatment with DMSO corresponds to '0'.
doi:10.1371/journal.pone.0048685.g002

Table 2. Effect of C29EA on HCV replication.

HCV strain (genotype)	EC_{50} (μg/ml)[a]	CC_{50} (μg/ml)[b]	SI[c]
Con 1 (1b)	1.5	>50	>33.3
JFH1 (2a)	24.9	>50	>2.3

[a]: Fifty percent effective concentration based on the inhibition of HCV replication.
[b]: Fifty percent cytotoxicity concentration based on the reduction of cell viability.
[c]: SI, selectivity index (CC_{50}/EC_{50}).
doi:10.1371/journal.pone.0048685.t002

Effect of C-29EA on NS3 Protease Activity

Serine protease and helicase domains are respectively located on the N-terminal and C-terminal portions of NS3 [32]. Thus, we examined the effect of C-29EA on NS3 protease activity by using an NS3 protease assay based on FRET. NS3/4A serine protease was mixed with various concentrations of C-29EA. The initial velocity at each concentration of C-29EA was calculated during a 120 min reaction. The initial velocity in the absence of C-29EA represented 100% of relative protease activity. C-29EA decreased the serine protease activity in a dose-dependent manner (Fig. 7). The IC_{50} of C-29EA was 10.9 μg/ml, which is similar to the value estimated by helicase assay. These results suggest that C-29EA includes the compound(s) inhibiting the protease activity of NS3 in addition to the helicase activity.

Combination Antiviral Activity of C-29EA and Interferon-alpha

Treatment with C-29EA may potentiate inhibitory action of interferon-alpha, since it inhibited the protease and helicase activities of NS3 but not induce the interferon response as described above. Then, we examined effect of treatment using both interferon and C-29EA on HCV replication. The replication

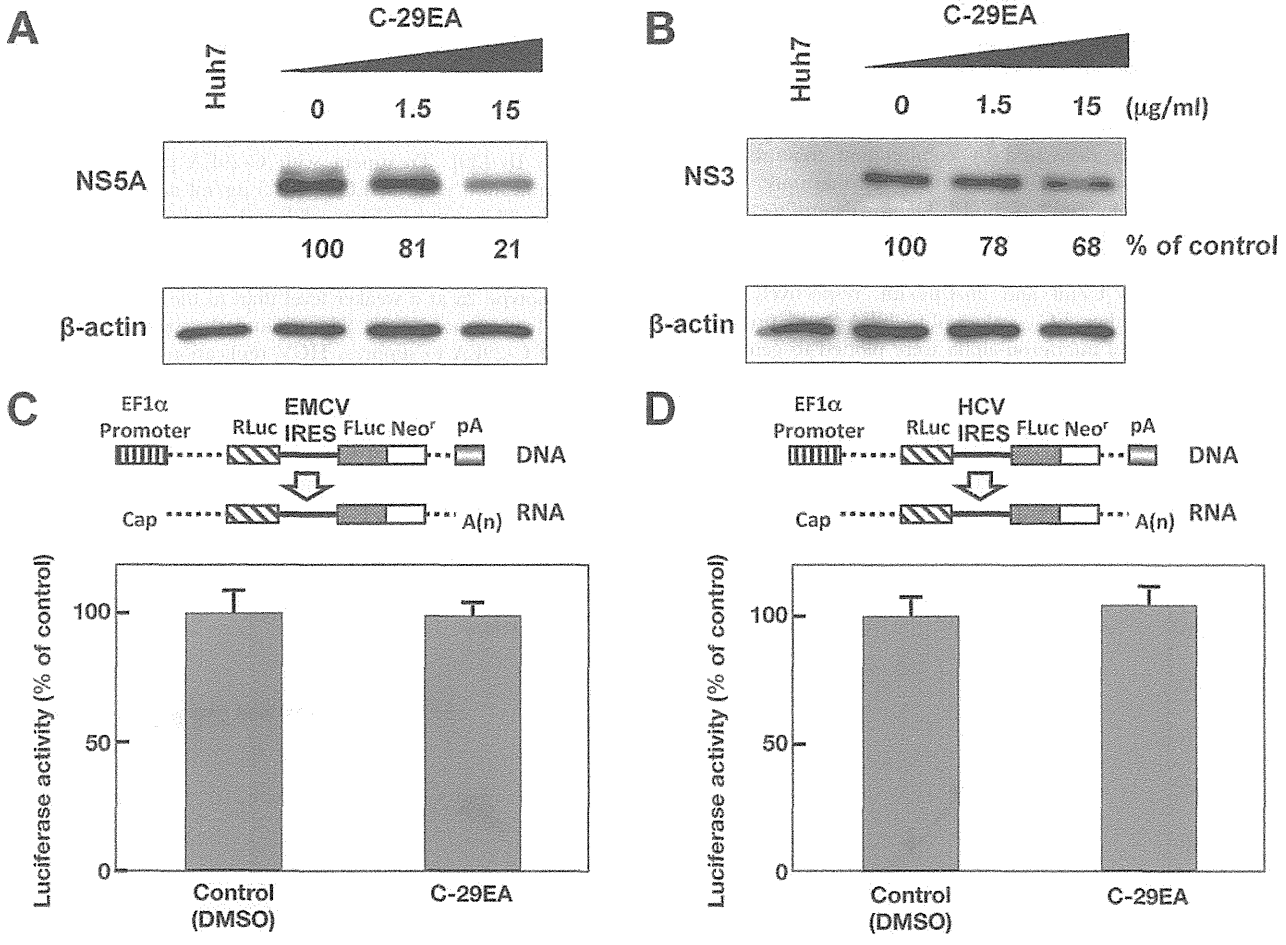

Figure 3. Effect of C-29EA on expression of viral proteins in replicon cell lines. The Huh7 replicon cell lines derived from genotype 1b (A) and 2a (B) were incubated with C-29EA at 37°C for 72 h. The treated cells were harvested and then subjected to Western blotting. Treatment with DMSO corresponds to '0'. The bicistronic gene is transcribed under the control of the elongation factor 1α (EF1α) promoter. The upstream cistron encoding *Renilla* luciferase (RLuc) is translated by a cap-dependent mechanism. The downstream cistron encodes the fusion protein (Feo), which consists of the firefly luciferase (Fluc) and neomycin phosphotransferase (Neo^r), and is translated under the control of the EMCV IRES (C) or HCV IRES (D). The Huh7 cell line transfected with the plasmid (each above the panel in C and D) was established in the presence of G418. The cells were incubated for 72 h without (control) and with 15 μg/ml of C-29EA. Firefly or *Renilla* luciferase activity was measured by the method described in Materials and Methods and was normalized by the protein concentration. F/R: relative ratio of firefly luciferase activity to *Renilla* luciferase activity. F/R is presented as a percentage of the control condition. Error bars indicate standard deviation. The data represent three independent experiments.
doi:10.1371/journal.pone.0048685.g003

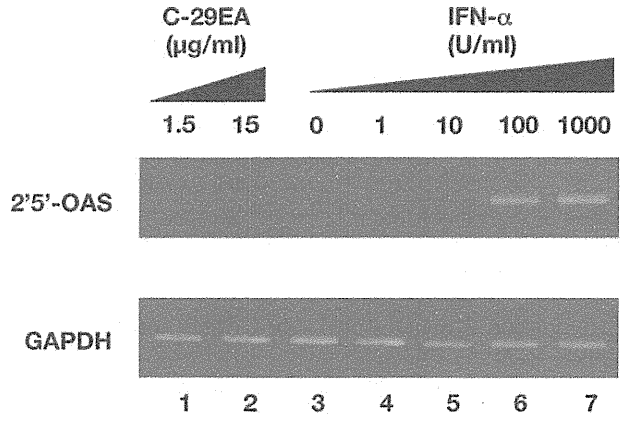

Figure 4. Effect of C-29EA on interferon signaling pathway. The Huh7 replicon cell line of genotype 1b was treated without (lane 3) or with 1, 10, 100, or 1000 U/mL interferon-alpha 2b (lanes 4–7), and 1.5 or 15 μg/ml C-29EA (lanes 1–2) for 48 h. Treatment with DMSO corresponds to '0'. The mRNAs of 2', 5'-OAS, and GAPDH as an internal control were detected by RT-PCR. Error bars indicate standard deviation. The data represent three independent experiments.
doi:10.1371/journal.pone.0048685.g004

of replicon was decreased in the presence of C-29EA or interferon-alpha and further decreased by combination treatment using interferon-alpha and C-29EA (Fig. 8A). Furthermore, we employed the isobologram method [33] to determine whether antiviral effect of the combination treatment exhibits additive or synergistic. EC_{90} values of interferon-alpha and C-29EA were estimated at 10.7 U/ml and 26.4 μg/ml, respectively, in the absence of each other. EC_{90} values of C-29EA in the presence of 0, 2.5 and 5 U/ml interferon-alpha were plotted to generate an isobole. Figure 8B shows that the isobole exhibits concave curvilinear, representing synergy but not additivity. These results suggest that combination treatment of interferon-alpha and C-29EA exhibits synergistic inhibition of HCV replication.

Discussion

Several natural products have been reported as anti-viral agents against HCV replication. Silbinin, epigallocatechin 3-gallate, and proanthocyanidins, which were prepared from milk thistle, green tea, and blueberry leaves, respectively, have exhibited inhibitory activity against HCV replication in cultured cells [34–37]. In our previous report, we identified manoalide as an anti-HCV agent from a marine sponge extract by high-throughput screening targeting NS3 helicase activity [38]. Manoalide inhibited ATPase, RNA binding, and NS3 helicase activity in enzymological assays. The EtOAc extract of the marine feather star also suppressed HCV replication in HCV replicon cell lines derived from genotype 1b, and it inhibited the RNA-binding activity but not the ATPase activity of NS3 helicase [30]. In this study, we screened 84 extracts of marine organisms for their ability to inhibit HCV replication in replicon cell lines and HCV cell culture system. Among these extracts, C-29EA, which was extracted from *Amphimedon* sp., most strongly inhibited HCV replication regardless of cytotoxicity. We previously reported that the EtOAc extract (SG1-23-1) of the feather star *Alloeocomatella polycladia* inhibited HCV replication with an EC_{50} of 22.9 to 44.2 μg/ml in HCV replicon cells derived from genotype 1b [30]. Treatment with C-29EA potently inhibited HCV replication with an EC_{50} of 1.5 μg/ml and with an SI of more than 33.3 in the replicon cell line derived from genotype 1b, regardless of cytotoxicity (Fig. 1B and Table 2). However, C-29EA exhibited an EC_{50} of 24.9 μg/ml in a replicon cell line derived from genotype 2a at a weaker level than in the replicon cell line derived from genotype 1b (Figs. 1 and 2), suggesting that the ability of C-29EA to suppress HCV replication is dependent on the viral genotype or strain.

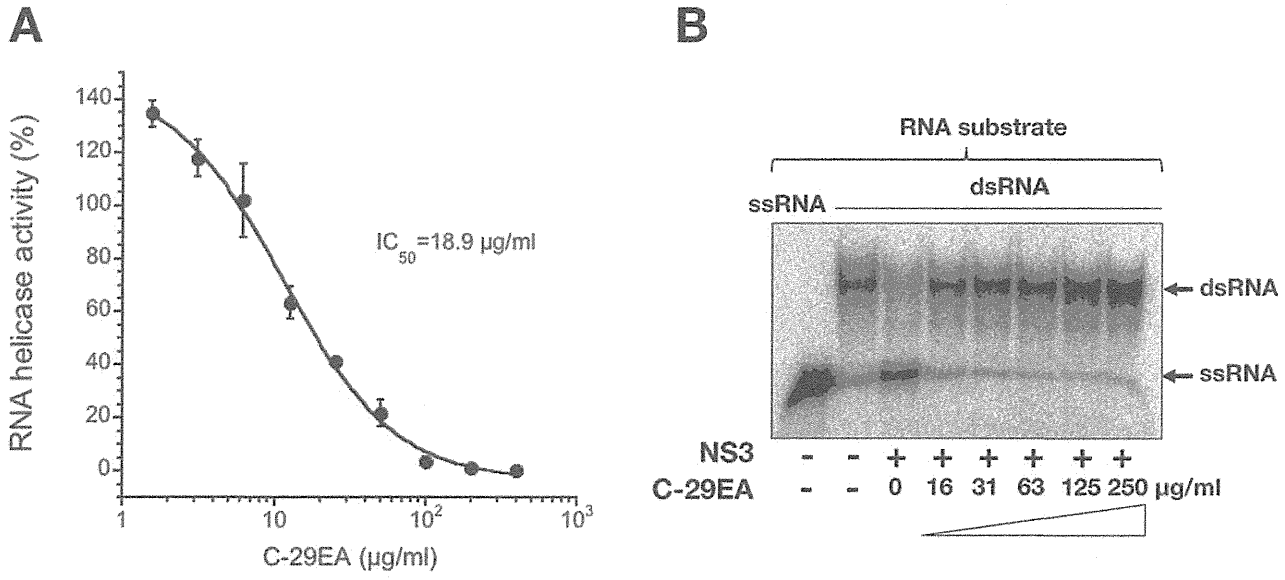

Figure 5. Effect of C-29EA on unwinding activity of NS3 helicase. (A) NS3 helicase activity was measured by PET assay. The reactions were carried out in the absence or presence of C-29EA. Helicase activity in the absence of C-29EA was defined as 100% helicase activity. Treatment with DMSO corresponds to '0'. The data are presented as the mean ± standard deviation for three replicates. (B) The unwinding activity of NS3 helicase was measured by an RNA unwinding assay using radioisotope-labeled RNA. The heat-denatured single-strand RNA (26-mer) and the partial duplex RNA substrate were applied to lanes 1 and 2, respectively. The duplex RNA was reacted with NS3 (300 nM) in the presence of C-29EA (lanes 4–9, 16–250 μg/ml). The resulting samples were subjected to native polyacrylamide gel electrophoresis. Treatment with DMSO corresponds to '0'.
doi:10.1371/journal.pone.0048685.g005

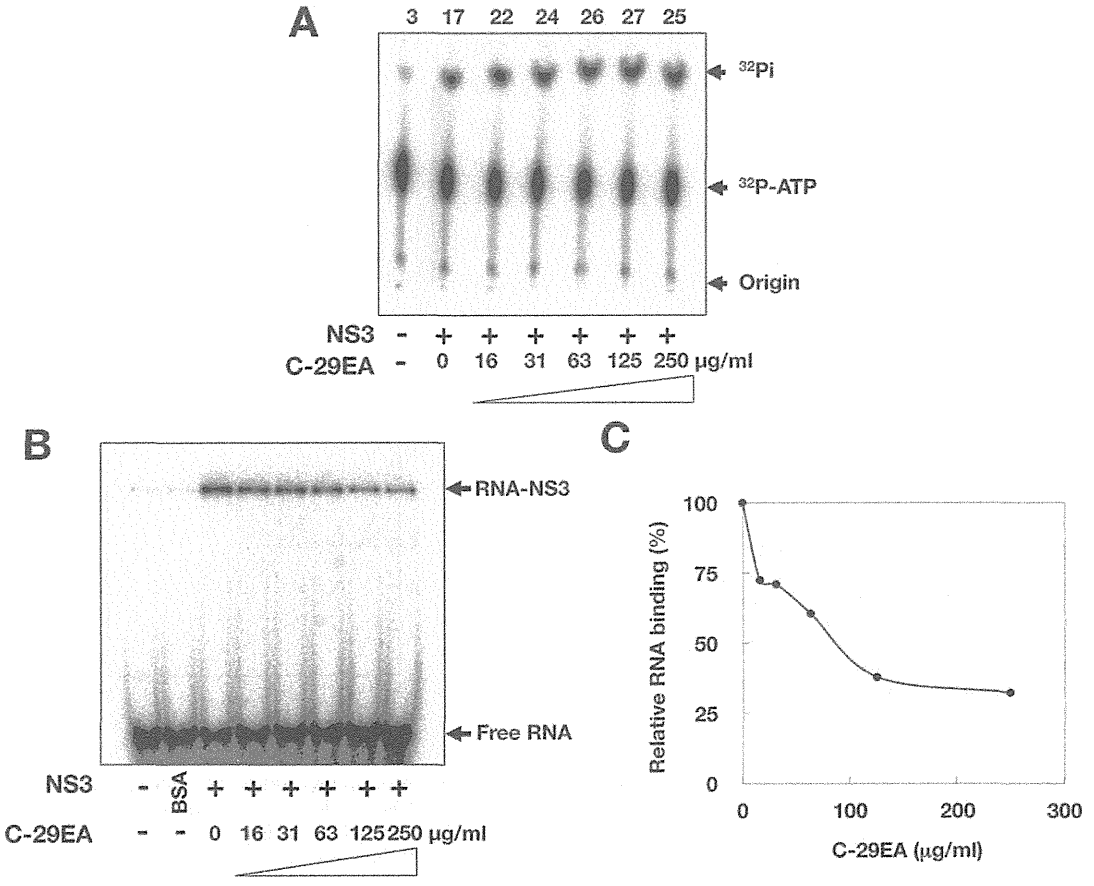

Figure 6. Effect of C-29EA on ATPase and RNA-binding activities of NS3 helicase. (A) The reaction mixtures were incubated with [γ-^{32}P] ATP as described in Materials and Methods. The reaction mixtures were subjected to thin-layer chromatography. The start positions and migrated positions of ATP and free phosphoric acid are indicated as 'Origin', '^{32}P-ATP', and '^{32}P-Pi', respectively, on the right side of the figure. The data represent three independent experiments. Treatment with DMSO corresponds to '0'. (B) Gel mobility shift assay for RNA-binding activity of NS3 helicase. The reaction was carried out with 0.5 nM labeled ssRNA at the indicated concentrations of C-29EA or DMSO. The reaction mixture was subjected to gel mobility shift assay. (C) The relative RNA-binding ability was calculated with band densities in each lane and presented as a percentage of RNA-NS3 in the total density. The data represent three independent experiments. Treatment with DMSO corresponds to '0'.
doi:10.1371/journal.pone.0048685.g006

HCV NS3 is well known to play a crucial role in viral replication through helicase and protease activities [5,39]. The N-terminal third of NS3 is responsible for serine protease activity in order to process the C-terminal portion of polyprotein containing viral nonstructural proteins [32]. The remaining portion of NS3 exhibits ATPase and RNA-binding activities responsible for helicase activity, which is involved in unwinding double-stranded RNA during replication of genomic viral RNA [40–42]. A negative-strand RNA is synthesized based on a viral genome (positive strand) after viral particles in the infected cells are uncoated, and is then used itself as a template to synthesize a positive-stranded RNA, which is translated or packaged into viral particles. Thus, both helicase and protease activities of NS3 are critical for HCV replication and could be targeted for the development of antiviral agents against HCV.

NS3 helicase activity was inhibited by treatment with C-29EA in a dose-dependent manner with an IC_{50} of 18.9 μg/ml (Fig. 5A). RNA-binding activity, but not ATPase activity, was inhibited by treatment with C-29EA (Fig. 6). Treatment with C-29EA did not significantly affect the HCV-IRES activity and did not induce interferon-stimulated gene 2′,5′-OAS (Figs. 3 and 4). Furthermore, the serine protease activity of NS3 was inhibited by using C-29EA with an IC_{50} of 10.9 μg/ml (Fig. 7). These results suggest that *Amphimedon* sp. includes the unknown compound(s) that could suppress NS3 enzymatic activity to inhibit HCV replication. Although the mechanism by which treatment with C-29EA could inhibit HCV replication has not yet been revealed, the unknown compound(s) may be associated with the inhibition of NS3 protease and helicase, leading to the suppression of HCV replication. However, other effects of extract C-29EA on HCV replication could not be excluded in this study.

The compound 1-N, 4-N-bis [4-(1H-benzimidazol-2-yl)phenyl] benzene-1,4-dicarboxamide, which is designated as $(BIP)_2B$, was reported to be a potent and selective inhibitor of HCV NS3 helicase [43]. This compound competitively decreases the binding ability of HCV NS3 helicase to nucleic acids. The compound $(BIP)_2B$ inhibited RNA-induced stimulation of ATPase, although it did not directly affect the ATP hydrolysis activity of NS3 helicase. Thus, $(BIP)_2B$ could not affect ATPase activity without RNA or with a high concentration of RNA. Treatment with C-29EA inhibited helicase activity and viral replication but not ATPase activity (Figs. 1B, 2, 5, and 6). This extract suppressed the binding of RNA to helicase but exhibited no suppression of ATPase by NS3 helicase. Thus, the inhibitory action of extract C-29EA seems

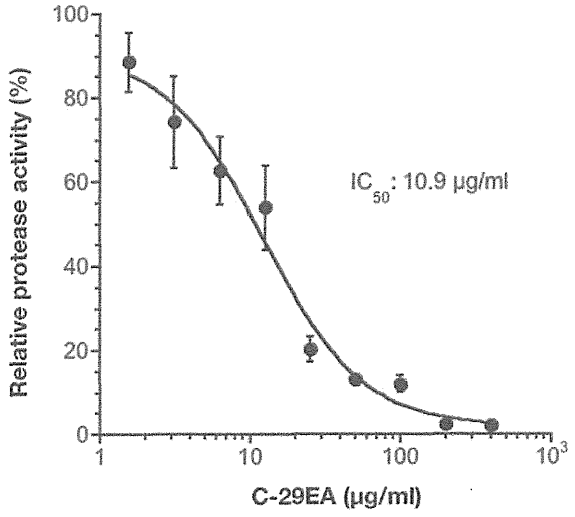

Figure 7. Effect of C-29EA on the activity of NS3 serine protease. NS3/4A serine protease was mixed with various concentrations of C-29EA or DMSO (0) in the reaction mixture and then incubated at 37°C for 120 min. The initial velocity at each concentration of C-29EA was calculated during 120 min reaction. The initial velocity in the absence of C-29EA was defined as 100% of relative protease activity. The data are presented as the mean ± standard deviation for three replicates.
doi:10.1371/journal.pone.0048685.g007

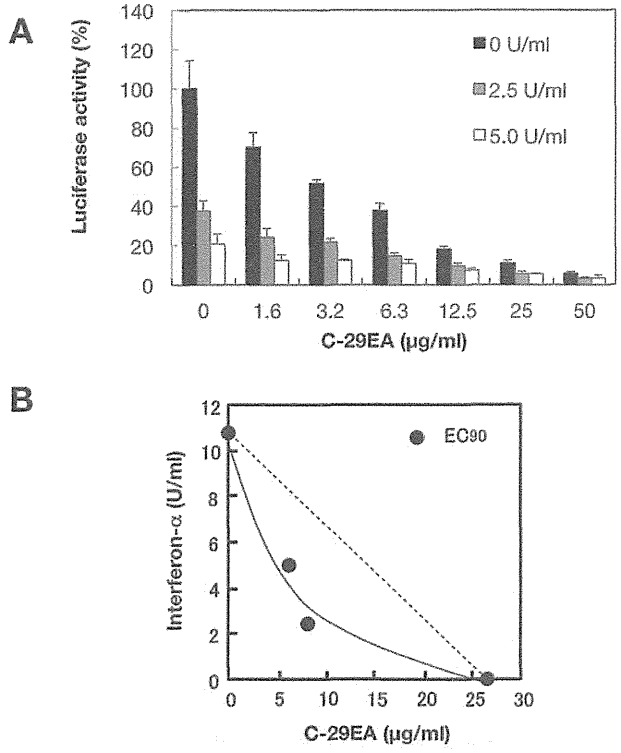

Figure 8. Effect of C-29EA on the antiviral activity of interferon-alpha. (A) The Huh7 cell line, including the subgenomic replicon RNA of genotype 1b strain Con1, was incubated in medium containing various concentrations of C-29EA or DMSO (0) in the presence or the absence of interferon-alpha. Luciferase assay were carried out as described in Materials and Methods. Error bars indicate standard deviation. The data represent three independent experiments. (B) Isobole plots of 90% inhibition of HCV replication. The broken line indicates the additive effect in the isobologram.
doi:10.1371/journal.pone.0048685.g008

different from that of $(BIP)_2B$. The quinolone derivative QU663 was reported to inhibit the unwinding activity of NS3 helicase by binding to an RNA-binding groove irrespective of its own ATPase activity [44]. The compound QU663 may competitively bind the RNA-binding site of NS3 but not affect ATPase activity, resulting in the inhibition of unwinding activity. In this study, treatment with C-29EA inhibited the RNA-binding activities of NS3 helicase but did not affect ATPase activity (Fig. 6). Furthermore, treatment with C-29EA suppressed the viral replication of HCV in an HCV cell culture system derived from several virus strains (Figs. 1 and 2, Table 2). The mechanism of C-29EA on the inhibition of NS3 helicase may be similar to that of compound QU663.

It is unknown whether one or several molecules included in C-29EA are critical for the inhibition of protease and helicase activities. The serine protease NS3/4A is one of the viral factors targeted for development into antiviral agents. Improvements in HCV therapy over the past several years have resulted in FDA approval of telaprevir (VX-950) [15,45] and boceprevir (SCH503034) [46,47]. Several studies suggest that the activities of NS3/4A protease and helicase in the full-length molecule enhance each other [48,49]. The NS3/4A protease has formed a complex with macrocyclic acylsulfonamide inhibitors [50,51]. Schiering et al. recently reported the structure of full-length NS3/4A in complex with a macrocyclic acylsulfonamide protease inhibitor [52], although the structure of full-length HCV NS3/4A in complex with a protease inhibitor has not been reported. The inhibitor binds to the active site of the protease, while the P4-capping and P2 moieties of the inhibitor are exposed toward the helicase interface and interact with both protease and helicase residues [52]. An unknown compound included in C-29EA might interact with both protease and helicase domains of NS3 to inhibit their activities. However, our data in this study have not excluded the possibility that several compounds included in C-29EA are related to the inhibition of protease and helicase of NS3/4A.

In conclusion, we showed that the EtOAc extract from *Amphimedon* sp. significantly inhibits HCV replication by suppressing viral helicase and protease activities. The purification of an inhibitory compound from the extract of *Amphimedon* sp. will be necessary in order to improve its efficacy by chemical modification.

Materials and Methods

Preparation of Extracts from Marine Organisms

All marine organisms used in this study were hand-collected by scuba diving off islands in Okinawa Prefecture, Japan. No specific permits were required for the described field studies. We do not have to obtain a local government permit to collect invertebrates except for stony corals and marine organisms for fisheries, which we did not collect in this study. The areas where we collected are not privately-owned or protected in any way. We did not collect any invertebrates listed in the red data book issued by Ministry of Environment, Japan. The sponges, tunicates, and soft corals used in this study are not listed at all. Hence, no specific permits are required for this collection in the same way as the previous report of Aratake et al. [53].

The sponge from which C-29EA was extracted was identified as *Amphimedon* sp. and deposited at Naturalis under the code RMNH POR 6100. Each specimen was soaked in acetone. The acetone-extract fraction prepared from each specimen was concentrated.

The resulting material was fractionated as an EtOAc- and water-soluble fraction. The water-soluble fraction was dried up and solubilized in MeOH. The EtOAc- and the MeOH-soluble fractions were used for screening. All samples were dried and then solubilized in dimethyl sulfoxide (DMSO) before testing.

Cell Lines and Virus

The following Huh-7-derived cell lines used in this study were maintained in Dulbecco's modified Eagle's medium containing 10% fetal calf serum and 0.5 mg/ml G418. The Lunet/Con1 LUN Sb #26 cell line, which harbors the subgenomic replicon RNA of the Con1 strain (genotype 1b), was kindly provided by Ralf Bartenschlager [26]. Huh7/ORN3-5B #24 cell line, which harbors the subgenomic replicon RNA of the O strain (genotype 1b) was reported previously [54] and used for screening in this study (Table 1). HCV replicon cell line derived from genotype 2a strain JFH1 was described previously [55]. The surviving cells were infected with the JFH-1 virus at a multiplicity of infection (moi) of 0.05. The viral RNA derived from the plasmid pJFH1 was transcribed and introduced into Huh7OK1 cells according to the method of Wakita et al. [56]. The infectivity of the JFH1 strain was determined by a focus-forming assay [56].

Quantitative Reverse-transcription PCR (qRT-PCR) and Estimation of Core Protein

The estimation of viral RNA genome was carried out by the method described previously [57] with slight modification. Total RNAs were prepared from cells and culture supernatants by using an RNeasy mini kit (QIAGEN, Tokyo, Japan) and QIAamp Viral RNA mini kit (QIAGEN), respectively. First-strand cDNA was synthesized by using a high capacity cDNA reverse transcription kit (Applied Biosystems, Carlsbad, CA, USA) with random primers. Each cDNA was estimated by using Platinum SYBR Green qPCR SuperMix UDG (Invitrogen, Carlsbad, CA, USA) according to the manufacturer's protocol. Fluorescent signals of SYBR Green were analyzed by using an ABI PRISM 7000 (Applied Biosystems). The HCV internal ribosomal entry site (IRES) region was amplified using the primer pair 5′-GAGTGTCGTGCAGCCTCCA -3′ and 5′- CACTCGCAAG-CACCCTATCA -3′. Expression of HCV core protein was determined by an enzyme-linked immunosorbent assay (ELISA) as described previously [57].

Determination of Luciferase Activity and Cytotoxicity in HCV Replicon Cells

HCV replicon cells were seeded at 2×10^4 cells per well in a 48-well plate 24 h before treatment. C-29EA was added to the culture medium at various concentrations. The treated cells were harvested 72 h post-treatment and lysed in cell culture lysis reagent (Promega, Madison, WI, USA) or *Renilla* luciferase assay lysis buffer (Promega). Luciferase activity in the harvested cells was estimated with a luciferase assay system (Promega) or a *Renilla* luciferase assay system (Promega). The resulting luminescence was detected by the Luminescencer-JNR AB-2100 (ATTO, Tokyo, Japan) and corresponded to the expression level of the HCV replicon. Cell viability was measured by a dimethylthiazol carboxymethoxy-phenylsulfophenyl tetrazolium (MTS) assay using a CellTiter 96 aqueous one-solution cell proliferation assay kit (Promega).

Effects on Activities of Internal Ribosome Entry Site (IRES)

Huh7 cells were transfected with pEF.Rluc.HCV.IRES.Feo or pEF.Rluc.EMCV.IRES.Feo and then were established in medium containing 0.25 mg/ml G418, as described previously [58]. These cell lines were seeded at 2×10^4 cells per well in a 48-well plate 24 h before treatment, treated with 15 μg/ml extract C-29EA, and then harvested at 72 h post-treatment. The firefly luciferase activities were measured with a luciferase assay system (Promega). The total protein concentration was measured using the BCA Protein Assay Reagent Kit (Thermo Scientific, Rockford, IL, USA) to normalize luciferase activity.

Western Blotting and Reverse-transcription Polymerase Chain Reaction (RT-PCR)

Western blotting was carried out by a method described previously [30]. The antibodies to NS3 (clone 8G-2, mouse monoclonal, Abcam, Cambridge, UK), NS5A (clone 256-A, mouse monoclonal, ViroGen, Watertown, MA, USA), and beta-actin were purchased from Cell Signaling Technology (rabbit polyclonal, Danvers, MA, USA) and were used as the primary antibodies in this study. RT-PCR was carried out by a method described previously [30,58].

Assays for RNA Helicase, ATPase, and RNA-binding Activities

A continuous fluorescence assay based on photoinduced electron transfer (PET) was described previously [29] and was slightly modified with regard to the reaction mixture [30]. The NS3 RNA unwinding assay was carried out by the method of Gallinari et al. [59] with slight modifications [30]. NS3 ATPase activity was determined by the method of Gallinari et al. [59] with slight modifications [30]. RNA binding to NS3 helicase was analyzed by a gel mobility shift assay [30,31]. The gene encoding NS3 helicase was amplified from the viral genome of genotype 1b and was introduced into a plasmid for the expression of a recombinant protein [38,60]. The radioactive band was visualized with the Image Reader FLA-9000 and quantified by Multi Gauge V 3.11 software.

NS3 Protease Assay

The fluorescence NS3 serine protease assay based on fluorescence resonance energy transfer (FRET) was carried out by the modified method using the SensoLyte^{TM} 520 HCV protease assay kit (AnaSpec, Fremont, CA, USA). In brief, NS3 protein with a two-fold excess of NS4A cofactor peptide (Pep4AK) was prepared in 1× assay buffer provided with the kit. HCV NS3/4A protease was mixed with increasing concentrations of C-29EA and incubated at 37°C for 15 min. The reaction was started by adding the 5-FAM/QXL 520 substrate to the reaction mixture containing 180 nM HCV NS3/4A protease and various concentrations (0–400 μg/ml) of C-29EA. The resulting mixture (20 μl) was incubated at 37°C for 120 min using a LightCycler 1.5 (Roche Diagnostics, Basel, Switzerland). The fluorescence intensity was recorded every minute for 120 min. The NS3 serine protease activity was calculated as the initial reaction velocity and presented as a percentage of relative activity to that of the control examined with DMSO solvent but not C-29EA, in the same way as described in the fluorescence helicase assay [29].

Analysis of Drug-drug Interaction

The effects of drug combinations were evaluated using the isobologram method [33]. Various doses of C-29EA and interferon-alpha on 90% inhibition of HCV replication were combined to generate an isoeffect curve (isobole) to determine drug–drug interaction. Concave, linear, and convex curves exhibit synergy, additivity, and antagonism, respectively.

Statistical Analysis

The results are expressed as the mean ± standard deviation. The significance of differences in the means was determined by Student's *t*-test.

Acknowledgments

We thank T. Wakita and R. Bartenschlager for kindly providing the virus, cell lines, and plasmids; and H. Kasai and I. Katoh for their helpful comments and discussions.

Author Contributions

Conceived and designed the experiments: MN MT YS ST NA NN AY JT KM. Performed the experiments: YF KAS AF YM OF HT AY. Analyzed the data: MI NK NS SM NE. Wrote the paper: YF AY JT KM. Collected marine organisms: JT. Identified the sponge: NJdV.

References

1. Baldo V, Baldovin T, Trivello R, Floreani A (2008) Epidemiology of HCV infection. Curr Pharm Des 14: 1646–1654.
2. Seeff LB (2002) Natural history of chronic hepatitis C. Hepatology 36: S35–46.
3. Moriishi K, Matsuura Y (2012) Exploitation of lipid components by viral and host proteins for hepatitis C virus infection. Front Microbiol 3: 54.
4. Tsukiyama-Kohara K, Iizuka N, Kohara M, Nomoto A (1992) Internal ribosome entry site within hepatitis C virus RNA. J Virol 66: 1476–1483.
5. Kim DW, Gwack Y, Han JH, Choe J (1995) C-terminal domain of the hepatitis C virus NS3 protein contains an RNA helicase activity. Biochem Biophys Res Commun 215: 160–166.
6. Kanai A, Tanabe K, Kohara M (1995) Poly(U) binding activity of hepatitis C virus NS3 protein, a putative RNA helicase. FEBS Lett 376: 221–224.
7. Manns MP, Wedemeyer H, Cornberg M (2006) Treating viral hepatitis C: efficacy, side effects, and complications. Gut 55: 1350–1359.
8. McHutchison JG, Everson GT, Gordon SC, Jacobson IM, Sulkowski M, et al. (2009) Telaprevir with peginterferon and ribavirin for chronic HCV genotype 1 infection. N Engl J Med 360: 1827–1838.
9. Zeuzem S, Hultcrantz R, Bourliere M, Goeser T, Marcellin P, et al. (2004) Peginterferon alfa-2b plus ribavirin for treatment of chronic hepatitis C in previously untreated patients infected with HCV genotypes 2 or 3. J Hepatol 40: 993–999.
10. Asselah T, Marcellin P (2011) New direct-acting antivirals' combination for the treatment of chronic hepatitis C. Liver Int 31 Suppl 1: 68–77.
11. Jazwinski AB, Muir AJ (2011) Direct-acting antiviral medications for chronic hepatitis C virus infection. Gastroenterol Hepatol (N Y) 7: 154–162.
12. Lange CM, Sarrazin C, Zeuzem S (2010) Review article: specifically targeted anti-viral therapy for hepatitis C - a new era in therapy. Aliment Pharmacol Ther 32: 14–28.
13. Hofmann WP, Zeuzem S (2011) A new standard of care for the treatment of chronic HCV infection. Nat Rev Gastroenterol Hepatol 8: 257–264.
14. Kwong AD, Kauffman RS, Hurter P, Mueller P (2011) Discovery and development of telaprevir: an NS3–4A protease inhibitor for treating genotype 1 chronic hepatitis C virus. Nat Biotechnol 29: 993–1003.
15. Jacobson IM, McHutchison JG, Dusheiko G, Di Bisceglie AM, Reddy KR, et al. (2011) Telaprevir for previously untreated chronic hepatitis C virus infection. N Engl J Med 364: 2405–2416.
16. Sarrazin C, Hezode C, Zeuzem S, Pawlotsky JM (2012) Antiviral strategies in hepatitis C virus infection. J Hepatol 56 Suppl 1: S88–100.
17. Chen ST, Wu PA (2012) Severe Cutaneous Eruptions on Telaprevir. J Hepatol 57: 470–472.
18. Kieffer TL, Kwong AD, Picchio GR (2010) Viral resistance to specifically targeted antiviral therapies for hepatitis C (STAT-Cs). J Antimicrob Chemother 65: 202–212.
19. Thompson AJ, McHutchison JG (2009) Antiviral resistance and specifically targeted therapy for HCV (STAT-C). J Viral Hepat 16: 377–387.
20. Chin YW, Balunas MJ, Chai HB, Kinghorn AD (2006) Drug discovery from natural sources. AAPS J 8: E239–253.
21. Koehn FE, Carter GT (2005) The evolving role of natural products in drug discovery. Nat Rev Drug Discov 4: 206–220.
22. Li JW, Vederas JC (2009) Drug discovery and natural products: end of an era or an endless frontier? Science 325: 161–165.
23. Donia M, Hamann MT (2003) Marine natural products and their potential applications as anti-infective agents. Lancet Infect Dis 3: 338–348.
24. Molinski TF, Dalisay DS, Lievens SL, Saludes JP (2009) Drug development from marine natural products. Nat Rev Drug Discov 8: 69–85.
25. Mayer AM, Glaser KB, Cuevas C, Jacobs RS, Kem W, et al. (2010) The odyssey of marine pharmaceuticals: a current pipeline perspective. Trends Pharmacol Sci 31: 255–265.
26. Frese M, Barth K, Kaul A, Lohmann V, Schwarzle V, et al. (2003) Hepatitis C virus RNA replication is resistant to tumour necrosis factor-alpha. J Gen Virol 84: 1253–1259.
27. Blight KJ, Kolykhalov AA, Rice CM (2000) Efficient initiation of HCV RNA replication in cell culture. Science 290: 1972–1974.
28. Guo JT, Bichko VV, Seeger C (2001) Effect of alpha interferon on the hepatitis C virus replicon. J Virol 75: 8516–8523.
29. Tani H, Akimitsu N, Fujita O, Matsuda Y, Miyata R, et al. (2009) High-throughput screening assay of hepatitis C virus helicase inhibitors using fluorescence-quenching phenomenon. Biochem Biophys Res Commun 379: 1054–1059.
30. Yamashita A, Salam KA, Furuta A, Matsuda Y, Fujita O, et al. (2012) Inhibition of hepatitis C virus replication and NS3 helicase by the extract of the feather star *Alloeocomatella polycladia*. Mar Drugs 10: 744–761.
31. Huang Y, Liu ZR (2002) The ATPase, RNA unwinding, and RNA binding activities of recombinant p68 RNA helicase. J Biol Chem 277: 12810–12815.
32. Failla C, Tomei L, De Francesco R (1994) Both NS3 and NS4A are required for proteolytic processing of hepatitis C virus nonstructural proteins. J Virol 68: 3753–3760.
33. Leu GZ, Lin TY, Hsu JT (2004) Anti-HCV activities of selective polyunsaturated fatty acids. Biochem Biophys Res Commun 318: 275–280.
34. Ahmed-Belkacem A, Ahnou N, Barbotte L, Wychowski C, Pallier C, et al. (2010) Silibinin and related compounds are direct inhibitors of hepatitis C virus RNA-dependent RNA polymerase. Gastroenterology 138: 1112–1122.
35. Ciesek S, von Hahn T, Colpitts CC, Schang LM, Friesland M, et al. (2011) The green tea polyphenol, epigallocatechin-3-gallate, inhibits hepatitis C virus entry. Hepatology 54: 1947–1955.
36. Takeshita M, Ishida Y, Akamatsu E, Ohmori Y, Sudoh M, et al. (2009) Proanthocyanidin from blueberry leaves suppresses expression of subgenomic hepatitis C virus RNA. J Biol Chem 284: 21165–21176.
37. Wagoner J, Negash A, Kane OJ, Martinez LE, Nahmias Y, et al. (2010) Multiple effects of silymarin on the hepatitis C virus lifecycle. Hepatology 51: 1912–1921.
38. Salam KA, Furuta A, Noda N, Tsuneda S, Sekiguchi Y, et al. (2012) Inhibition of Hepatitis C Virus NS3 Helicase by Manoalide. J Nat Prod 75: 650–654.
39. Bartenschlager R, Ahlborn-Laake L, Mous J, Jacobsen H (1993) Nonstructural protein 3 of the hepatitis C virus encodes a serine-type proteinase required for cleavage at the NS3/4 and NS4/5 junctions. J Virol 67: 3835–3844.
40. Belon CA, Frick DN (2009) Helicase inhibitors as specifically targeted antiviral therapy for hepatitis C. Future Virol 4: 277–293.
41. Frick DN (2007) The hepatitis C virus NS3 protein: a model RNA helicase and potential drug target. Curr Issues Mol Biol 9: 1–20.
42. Kwong AD, Rao BG, Jeang KT (2005) Viral and cellular RNA helicases as antiviral targets. Nat Rev Drug Discov 4: 845–853.
43. Belon CA, High YD, Lin TI, Pauwels F, Frick DN (2010) Mechanism and specificity of a symmetrical benzimidazolephenylcarboxamide helicase inhibitor. Biochemistry 49: 1822–1832.
44. Maga G, Gemma S, Fattorusso C, Locatelli GA, Butini S, et al. (2005) Specific targeting of hepatitis C virus NS3 RNA helicase. Discovery of the potent and selective competitive nucleotide-mimicking inhibitor QU663. Biochemistry 44: 9637–9644.
45. Reesink HW, Zeuzem S, Weegink CJ, Forestier N, van Vliet A, et al. (2006) Rapid decline of viral RNA in hepatitis C patients treated with VX-950: a phase Ib, placebo-controlled, randomized study. Gastroenterology 131: 997–1002.
46. Malcolm BA, Liu R, Lahser F, Agrawal S, Belanger B, et al. (2006) SCH 503034, a mechanism-based inhibitor of hepatitis C virus NS3 protease, suppresses polyprotein maturation and enhances the antiviral activity of alpha interferon in replicon cells. Antimicrob Agents Chemother 50: 1013–1020.
47. Njoroge FG, Chen KX, Shih NY, Piwinski JJ (2008) Challenges in modern drug discovery: a case study of boceprevir, an HCV protease inhibitor for the treatment of hepatitis C virus infection. Acc Chem Res 41: 50–59.
48. Beran RK, Pyle AM (2008) Hepatitis C viral NS3–4A protease activity is enhanced by the NS3 helicase. J Biol Chem 283: 29929–29937.
49. Beran RK, Serebrov V, Pyle AM (2007) The serine protease domain of hepatitis C viral NS3 activates RNA helicase activity by promoting the binding of RNA substrate. J Biol Chem 282: 34913–34920.
50. Cummings MD, Lindberg J, Lin TI, de Kock H, Lenz O, et al. (2010) Induced-fit binding of the macrocyclic noncovalent inhibitor TMC435 to its HCV NS3/NS4A protease target. Angew Chem Int Ed Engl 49: 1652–1655.
51. Romano KP, Ali A, Royer WE, Schiffer CA (2010) Drug resistance against HCV NS3/4A inhibitors is defined by the balance of substrate recognition versus inhibitor binding. Proc Natl Acad Sci U S A 107: 20986–20991.
52. Schiering N, D'Arcy A, Villard F, Simic O, Kamke M, et al. (2011) A macrocyclic HCV NS3/4A protease inhibitor interacts with protease and helicase residues in the complex with its full-length target. Proc Natl Acad Sci U S A 108: 21052–21056.

53. Aratake S, Tomura T, Saitoh S, Yokokura R, Kawanishi Y, et al. (2012) Soft coral Sarcophyton (Cnidaria: Anthozoa: Octocorallia) species diversity and chemotypes. PLoS One 7: e30410.
54. Ikeda M, Abe K, Dansako H, Nakamura T, Naka K, et al. (2005) Efficient replication of a full-length hepatitis C virus genome, strain O, in cell culture, and development of a luciferase reporter system. Biochem Biophys Res Commun 329: 1350–1359.
55. Nishimura-Sakurai Y, Sakamoto N, Mogushi K, Nagaie S, Nakagawa M, et al. (2010) Comparison of HCV-associated gene expression and cell signaling pathways in cells with or without HCV replicon and in replicon-cured cells. J Gastroenterol 45: 523–536.
56. Wakita T, Pietschmann T, Kato T, Date T, Miyamoto M, et al. (2005) Production of infectious hepatitis C virus in tissue culture from a cloned viral genome. Nat Med 11: 791–796.
57. Moriishi K, Shoji I, Mori Y, Suzuki R, Suzuki T, et al. (2010) Involvement of PA28gamma in the propagation of hepatitis C virus. Hepatology 52: 411–420.
58. Jin H, Yamashita A, Maekawa S, Yang P, He L, et al. (2008) Griseofulvin, an oral antifungal agent, suppresses hepatitis C virus replication in vitro. Hepatol Res 38: 909–918.
59. Gallinari P, Brennan D, Nardi C, Brunetti M, Tomei L, et al. (1998) Multiple enzymatic activities associated with recombinant NS3 protein of hepatitis C virus. J Virol 72: 6758–6769.
60. Nishikawa F, Funaji K, Fukuda K, Nishikawa S (2004) In vitro selection of RNA aptamers against the HCV NS3 helicase domain. Oligonucleotides 14: 114–129.

Journal of proteome research

Article

pubs.acs.org/jpr

Proteomic Analysis of Hepatitis C Virus (HCV) Core Protein Transfection and Host Regulator PA28γ Knockout in HCV Pathogenesis: A Network-Based Study

Lokesh P. Tripathi,[†,∥] Hiroto Kambara,[‡,∥] Kohji Moriishi,[‡] Eiji Morita,[‡] Takayuki Abe,[‡] Yoshio Mori,[‡] Yi-An Chen,[†,§] Yoshiharu Matsuura,[‡] and Kenji Mizuguchi*[,†,§]

[†]National Institute of Biomedical Innovation, 7-6-8 Saito Asagi, Ibaraki, Osaka, 567-0085, Japan

[‡]Department of Molecular Virology, Research Institute for Microbial Diseases and [§]Graduate School of Frontier Biosciences, Osaka University, 3-1 Yamada-Oka, Suita, Osaka, 565-0871, Japan

Supporting Information

ABSTRACT: Hepatitis C virus (HCV) causes chronic liver disease worldwide. HCV Core protein (Core) forms the viral capsid and is crucial for HCV pathogenesis and HCV-induced hepatocellular carcinoma, through its interaction with the host factor proteasome activator PA28γ. Here, using BD-PowerBlot high-throughput Western array, we attempt to further investigate HCV pathogenesis by comparing the protein levels in liver samples from Core-transgenic mice with or without the knockout of PA28γ expression (abbreviated PA28γ$^{-/-}$CoreTG and CoreTG, respectively) against the wild-type (WT). The differentially expressed proteins integrated into the human interactome were shown to participate in compact and well-connected cellular networks. Functional analysis of the interaction networks using a newly developed data warehouse system highlighted cellular pathways associated with vesicular transport, immune system, cellular adhesion, and cell growth and death among others that were prominently influenced by Core and PA28γ in HCV infection. Follow-up assays with *in vitro* HCV cell culture systems validated VTI1A, a vesicular transport associated factor, which was upregulated in CoreTG but not in PA28γ$^{-/-}$CoreTG, as a novel regulator of HCV release but not replication. Our analysis provided novel insights into the Core-PA28γ interplay in HCV pathogenesis and identified potential targets for better anti-HCV therapy and potentially novel biomarkers of HCV infection.

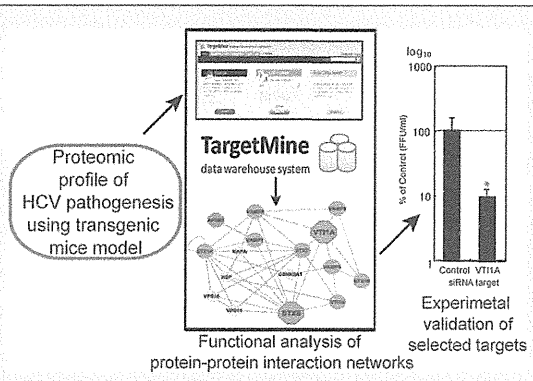

KEYWORDS: *CoreTG, GO, HCC, HCV, KEGG, OMIM, PA28γ$^{-/-}$CoreTG, PPI, siRNA, TargetMine*

INTRODUCTION

Hepatitis C virus (HCV) is a prime cause of chronic liver disease frequently characterized by liver inflammation with accompanying steatosis, progressive fibrosis, and hepatocellular carcinoma (HCC) and infects nearly 3% of the world's population. HCV contains a single-stranded RNA genome encoding a 3000-amino-acid polyprotein, which is processed by host and viral factors to yield 10 viral proteins, Core, E1, E2, p7, NS2, NS3, NS4A, NS4B, NS5A, and NS5B.[1−4] HCV variants are classified into six major genotypes with multiple subtypes characterized by phylogenetic heterogeneity, differences in infectivity, and interferon sensitivity.[5,6] The availability of cell-culture-based systems for HCV infection has provided an increased understanding of HCV pathogenesis.[5,7−9] Transgenic mice (preferably C57BL strain) expressing HCV proteins in the liver are also a preferred choice for the investigation of HCV pathogenesis.[10] However, despite considerable research efforts, precise molecular mechanisms underlying HCV pathology remain unclear.

HCV Core protein (hereafter referred to as Core) is spliced from the polyprotein by the signal peptidase and further processed into a highly conserved 21-kDa mature form by the signal peptide peptidase; this processing facilitates its transfer to the detergent-resistant membrane fraction where virus replication and assembly take place. Core is a multifunctional protein implicated in RNA binding and as a pathogenic factor; it induces steatosis and HCC and, thus, liver failure.[1,10] The ubiquitin-proteasome pathway, the premier intracellular protein degradation system in eukaryotes, is a key regulator of cellular processes and is also associated with the evasion of host immune response by many viruses, viral maturation, and progeny release.[11] Core binds to the proteasome activator PA28γ in the nucleus and is degraded via a PA28γ-dependent pathway. PA28γ plays a crucial role in Core-induced insulin resistance, steatogenesis, and hepatocarcinogenesis and in HCV propagation; PA28γ knockout in Core transgenic mice disrupts

Received: February 7, 2012
Published: May 31, 2012

steatosis and HCC, restores insulin sensitivity, and impairs viral particle production, and thus PA28γ is a promising target for anti-HCV therapies with minimal side effects.[2,12−15] However, the exact mechanisms through which PA28γ facilitates Core-induced HCV pathogenesis remain poorly understood.

In this study, we aim to put forth biological networks that describe the differential expression of the host proteins and their likely roles in modulating PA28γ function in HCV pathogenesis. We employed PowerBlot Western Array screening system, a high-throughput Western blotting method, to identify changes at the proteome level in Core expressing transgenic C57BL/6 mice with or without the knockout of PA28γ gene expression (abbreviated PA28$\gamma^{-/-}$CoreTG and CoreTG, respectively). In our analysis, we included human protein interaction data and gene regulatory information for the differentially expressed proteins using TargetMine, an integrated data warehouse that we have developed recently.[16] Our network-based analyses of the proteomic changes from the three data sets (CoreTGvsC57BL/6, PA28$\gamma^{-/-}$CoreTGvsC57BL/6 and PA28$\gamma^{-/-}$CoreTGvsCoreTG) provided novel insights into PA28γ function in Core-induced HCV pathogenesis. Furthermore, we identified VTI1A, a vesicular transport associated factor, which was upregulated in CoreTG but not in PA28$\gamma^{-/-}$CoreTG, as a novel regulator of HCV release and, thus, an attractive target for anti-HCV therapy.

MATERIALS AND METHODS

Protein Sample Preparation

Protein samples were prepared from the livers of the C57BL/6 wild-type (hereafter referred to as WT) and the transgenic mice expressing HCV Core protein genotype 1b line C49 with (PA28$\gamma^{-/-}$CoreTG) or without (CoreTG) the knockout of PA28γ expression.[2,12] Livers were harvested from three individuals each of WT, CoreTG, and PA28$\gamma^{-/-}$CoreTG mice, and the harvested samples for each mice type were pooled together prior to protein sample preparation for PowerBlot analysis. The pooled liver samples of each mice type were homogenized in 1x sample buffer of SDS-PAGE on ice and then boiled for 5 min. The boiled sample was sonicated for the viscosity of DNA and employed for PowerBlot analysis.

PowerBlot Western Array Analysis

The levels of differentially expressed proteins were determined by the PowerBlot assay by BD Biosciences Pharmingen (San Diego, CA, USA). Briefly, samples containing 200 μg of protein was loaded in one big well on top of a 4−15% gradient SDS-polyacrylamide gel and separated by electrophoresis (1.5 h at 150v). The proteins were transferred to Immobilon-FL membrane (Millipore, Billerica, MA, USA) for 2 h at 200 mA. After transfer, the membranes were incubated in the blocking buffer (LI-COR, Lincoln, NE, USA). The membrane was clamped with a Western blotting manifold that isolates 41 channels across the membrane. Each channel was incubated with a complex antibody cocktail for 1 h. The blots were removed from the manifold, washed, and hybridized for 30 min with secondary goat anti-mouse antibody conjugated to Alexa680 fluorescent dye (Molecular Probes, Eugene, OR, USA). Image data were captured using the Odyssey Infrared Imaging System (LI-COR). Data analysis included the raw and normalized signal intensity data from each blot. The results were expressed as fold change that represented the protein changes, either increasing or decreasing in the comparative analysis between the experimental samples and the control. The detected protein expression changes were listed in the order of confidence, 0 through 3, with 3 being the highest level of confidence, based on the signal quality. Only the data from confidence levels 2 and 3 (good quality signals; Supporting Information; Tables S1, S2a, S2b, and S2c) for proteins mapped to valid accessions were considered for further analysis. Proteins that displayed >1.8-fold change in abundance were judged to be differentially expressed, following the manufacturer's recommendation.

Human Orthologues for the Differentially Expressed Proteins

BD PowerBlot assay employs a cocktail of monoclonal antibodies that target human, mouse, and rat proteins, and in a specific study, over 90% were found to cross-react with proteins from human, mouse and rat[17] (Table S1). Human orthologues for the proteins picked up by the antibody cocktail were retrieved from KEGG (Tables S2a, S2b, and S2c).

Construction of Protein−Protein Interaction Networks

PPIs for the human orthologues of each set of differentially expressed proteins were retrieved from BioGRID 3.1.74[18] and iRefIndex 8.0[19] databases along with the interactions between the primary interactors of the differentially expressed proteins using TargetMine.[16] TargetMine is an integrated data warehouse that combines different biological data types and employs an objective protocol to prioritize candidate genes for further experimental investigation.[16] The interactions were merged and filtered for redundancy to infer overall extended PPI networks. Protein identifiers used in the different databases were mapped to Entrez gene IDs and official gene symbols. The official gene symbols are used hereafter, to refer to the differentially expressed proteins (Table 1) and their interacting partners. All the relationships discussed should be interpreted as protein relationships unless otherwise clarified.

PPI Network Topological Analysis

Network components were visualized using Cytoscape 2.6,[20] while network properties such as *node degree distribution* and *shortest path* measures were computed using the Cytoscape NetworkAnalyzer plugin[21] as described previously.[22] In a PPI network, the degree of a node (protein) is defined as the number of nodes directly connected to (interacting with) it, i.e., its first neighbors. *Node degree distribution*, $P(k)$, is the number of nodes with a degree k for $k = 0, 1, 2, \ldots$. The *shortest path length* between two nodes n and m, $L(n,m)$, is the minimal number of interactions that link proteins n and m in a PPI network. The *shortest path length distribution* is the number of node pairs (n,m) with $L(n,m) = x$ for $x = 1, 2, \ldots$. The *average shortest path length*, also known as the *characteristic path length*, gives the expected distance between two connected nodes i.e. the minimal number of interactions that link any two proteins in a PPI network.

Functional Analysis by Characterization of Enriched Biological Associations

Gene ontology (GO) associations retrieved from GO consortium,[23] biological pathway data from KEGG (retrieved on March 1, 2011),[24] and disease phenotype associations from OMIM[25] were used to assign functional annotations to the constituents of the extended PPI networks. The proteins in each of the extended PPI networks were uploaded to TargetMine to create protein lists, and the enrichment of specific biological themes (GO terms, KEGG Pathways, OMIM phenotypes) associated with each PPI network was estimated